# Argonne Aational Laboratory REACTOR DEVELOPMENT PROGRAM PROGRESS REPORT

October 1961

#### LEGAL NOTICE

This report was prepared as an account of Government sponsored work. Neither the United States, nor the Commission, nor any person acting on behalf of the Commission:

- A. Makes any warranty or representation, expressed or implied, with respect to the accuracy, completeness, or usefulness of the information contained in this report, or that the use of any information, apparatus, method, or process disclosed in this report may not infringe privately owned rights; or
- B. Assumes any liabilities with respect to the use of, or for damages resulting from the use of any information, apparatus, method, or process disclosed in this report.

As used in the above, "person acting on behalf of the Commission" includes any employee or contractor of the Commission, or employee of such contractor, to the extent that such employee or contractor of the Commission, or employee of such contractor prepares, disseminates, or provides access to, any information pursuant to his employment or contract with the Commission, or his employment with such contractor.

ANL-6454
Reactor Technology
(TID-4500, 16th Ed.,
Amended)
AEC Research and
Development Report

## ARGONNE NATIONAL LABORATORY 9700 South Cass Avenue Argonne, Illinois

## REACTOR DEVELOPMENT PROGRAM PROGRESS REPORT

October 1961

N. Hilberry, Laboratory Director

Division	Director
Chemical Engineering	S. Lawroski
Idaho	M. Novick
Metallurgy	F. G. Foote
Reactor Engineering	B. I. Spinrad
Remote Control	R. C. Goertz

Report coordinated by R. M. Adams

Issued November 15, 1961

Operated by The University of Chicago under Contract W-31-109-eng-38



#### FOREWORD

The Reactor Development Program Progress Report, issued monthly, is intended to be a means of reporting those items of significant technical progress which have occurred in both the specific reactor projects and the general engineering research and development programs. The report is organized in a way which, it is hoped, gives the clearest, most logical over-all view of progress. The budget classification is followed only in broad outline, and no attempt is made to report separately on each sub-activity number. Further, since the intent is to report only items of significant progress, not all activities are reported each month. In order to issue this report as soon as possible after the end of the month editorial work must necessarily be limited. Also, since this is an informal progress report, the results and data presented should be understood to be preliminary and subject to change unless otherwise stated.

The issuance of these reports is not intended to constitute publication in any sense of the word. Final results either will be submitted for publication in regular professional journals or will be published in the form of ANL topical reports.

### The last six reports issued in this series are:

April 1961	ANL-6355
May 1961	ANL-6374
June 1961	ANL-6387
July 1961	ANL-6399
August 1961	ANL-6409
September 1961	ANL-6433

#### TABLE OF CONTENTS

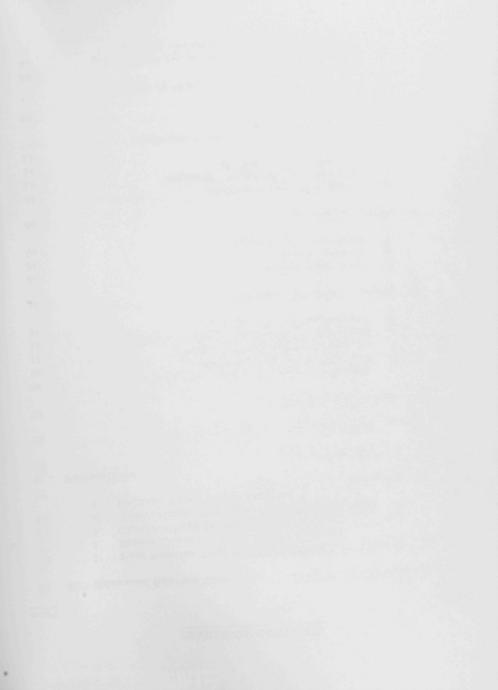
				Page
I.	Wat	er C	cooled Reactors (040101)	1
	A.	Gen	eral Research and Development	1
		1.	$ \label{eq:continuous}                                   $	1
	В.	EBV	WR	2
		1. 2.	100-Mw Modifications Experimental Equipment	2 3
	C.	вон	RAX-V	4
		1. 2. 3. 4.	Installation of Reactor and Components Procurement and Fabrication Design Development and Testing	4 6 7 8
II.	Sod	ium	Cooled Reactors (040103)	12
	A.	Gen	eral Research and Development	12
		1. 2. 3.	ZPR-III Experiments ZPR-III Analysis ZPR-VI	12 15 15
	В.	EBI	R-I	16
		1.	Fabrication of Core IV Fuel Elements	16
	C.	EBI	R-II	17
		1. 2. 3. 4. 5. 6.	Reactor Operation - Dry Critical Experiments Sodium Boiler Plant Power Plant Instrumentation and Controls Component Development - Steam Generators Component Development - Fuel Reprocessing	17 18 19 19 20
		7. 8.	Facilities Process Development Fuel Development - Core II	20 22 24

#### TABLE OF CONTENTS

			Page
III.	Rea	ctor Safety (040117)	26
	A.	Thermal Reactor Safety Studies	26
		<ol> <li>Fuel-Coolant Chemical Reactions</li> <li>Metal Oxidation and Ignition Studies</li> </ol>	26 26
	В.	Fast Reactor Safety Studies	28
		1. TREAT Program	28
IV.	Nuc	clear Technology and General Support (040400)	30
	Α.	Applied Nuclear Physics	30
		<ol> <li>High Conversion Critical Experiment</li> <li>Fast Spectrum Measurements</li> <li>Argonne Thermal Source Reactor</li> <li>Mathematical Numerical Methods Analysis</li> <li>Theoretical Reactor Physics</li> </ol>	30 30 31 31 32
	в.	Reactor Fuels Development	34
		<ol> <li>Corrosion Studies</li> <li>Ceramic Fuels</li> <li>Nondestructive Testing</li> </ol>	34 35 40
	C.	Heat Engineering	42
		<ol> <li>Double Tube Burnout Study</li> <li>Hydrodynamic Computer Program</li> <li>Hydrodynamic Instability</li> <li>Critical Heat Flux Survey</li> <li>Boiling from a Liquid-Liquid Interface</li> </ol>	42 42 42 43 43
	D.	Separations Processes	44
		<ol> <li>Fluidization and Fluoride Volatility Separations Processes</li> <li>General Chemistry and Chemical Engineering</li> <li>Chemical-Metallurgical Process Studies</li> </ol>	44 46 47
		J. Chemical-Metallurgical Process Studies	41

#### TABLE OF CONTENTS

			Page
	E. A	dvanced Reactor Concepts	49
	1.	Fast Reactor Test Facility (FARET)	49
	2.	Direct Conversion for Mobile Systems	51
	3.	Compact High Density Reactors	52
	4.	Supercritical Pressure Water Reactor Study	52
	5.	Organic Vapor Cycle Analysis	53
v.	Public	ations	54



#### I. WATER COOLED REACTORS (040101)

#### A. General Research and Development

#### 1. Irradiation of UO2 Pellets with Collapsed Aluminum Alloy Cladding

A three-rod prototype fuel element consisting of  $UO_2$  pellets in collapsed A-288 aluminum alloy tubing has been removed from the ANL-2 High Pressure Water Loop at MTR for an interim hot cell examination. Designation of the element is ANL-2-13. Each of the three rods in the element is 16 in. long and contains a column of  $UO_2$  pellets (0.321 in. diameter, 3.05% enriched) which have a density 95% of theoretical. The wrought A-288 aluminum alloy (1 w/o Ni, 0.5 w/o Fe, 0.1 w/o Ti, <20 ppm Si) tubing used for cladding has an O.D. of 0.385 in. with a wall thickness of 0.030 in. One rod contains square end pellets with a 0.001 in. thick annular gap filled with helium. Another rod contains square end pellets with zero gap prior to irradiation. This was accomplished by hydrostatically collapsing the tube on the pellets before irradiation. The third rod contains pellets with dished ends and an annular helium-filled gap 0.001 in. thick.

It was expected that the cladding would collapse onto the fuel pellets under the experimental conditions in the loop. However, in order to make the test as stringent as possible the cladding was collapsed on the one tube as described above prior to insertion in the loop.

The irradiation conditions are given in Table I.

## Table I. <u>Irradiation Conditions for</u> Aluminum Alloy Cladding

Bulk Coolant Temperature	240°C
Coolant Velocity	22.4 ft/sec
Coolant pH	5.0
Coolant Pressure	590 psig
Maximum Heat Flux	672,000 BTU/hr-ft
Maximum Integral $k(\theta) d\theta$	50 w/cm
Maximum Burnup	6100 Mwd/MT

Under the above conditions the aluminum alloy tubing did in fact collapse on all three columns of pellets as desired, and nucleate boiling occurred on the elements over a length of 4.3 in. Collapsed cladding results in intimate contact between the oxide fuel and cladding. This situation, coupled with the large difference in thermal expansion coefficients of aluminum and  $\rm UO_2$ , could lead in theory to separation of the pellets by thermal ratcheting and, ultimately, failure of the cladding. Because of these considerations, high strength sintered aluminum powder product tubing is commonly specified for  $\rm UO_2$  rods clad with aluminum in order to keep the pellets in a "free-standing" condition.

The potential advantages of wrought tubing over high strength sintered aluminum powder product tubing are so great, however, that a series of irradiations are in progress to determine by direct experiment whether or not wrought tubing can be used in pressurized boiling water. The principal advantages of wrought tubing are that it can be made much more cheaply than the powder metallurgy tubing, leak-tight welds can be made more easily, and its corrosion resistance is more reliable.

During the three months that the element was under irradiation no fission product activity release or other difficulty appeared. An identical element has been examined which was in an out-of-pile section of the loop during the test. This element was subjected to the same water conditions, pressures, etc., as the in-pile element. No dimensional changes of significance occurred in this element.

The above results indicate in a preliminary fashion that the use of  $\rm UO_2$  pellets in collapsed aluminum cladding may be a feasible approach to lower fuel fabrication costs for both water cooled and organic cooled reactors.

#### B. EBWR

#### 1. 100-MW Modifications

- a. Reboilers The primary reboilers were received October 17, 1961. Setting of the reboilers on their supports was completed October 19, 1961, and piping has begun. It is expected that the reboilers will be completely reinstalled before the end of November. Thereafter, hydrostatic tests will be performed to establish the integrity of the piping and to check the leak tightness of the tubes.
- b. Storage Rack (for Spike Fuel Assemblies) The storage rack has been completed and installed in the storage pit in EBWR. It can accommodate an entire EBWR core loading.
- c. Zircaloy-2 Follower Control Rods All of the Zircaloy-2 followers have been corrosion tested at 485°F for two weeks. Spot welds not made according to specifications show indications of corrosion product as was indicated in the August Progress Report (ANL-6409). The fusion welds in general appear sound; however, some corrosion product is noted on several of the welds in the heat affected zone.

As noted in the September Progress Report (ANL-6433) the first heat treated poison section distorted severely and could not be cold straightened. A new heat treatment has been investigated and requests for bids are now being sent out for processing nine rods to this heat treatment.

#### 2. Experimental Equipment

- a. <u>EBWR Instrumented Fuel Assemblies</u> A series of preliminary hydrodynamic runs with the riser section removed were made to check out the operation of the instrumented fuel assembly. The turbine flowmeters were found to be operating satisfactorily but several bad thermocouple connections in the secondary seals prevented the taking of subcooling measurements. These connections have been repaired and the thermocouples now appear to be functioning properly. The results obtained from the initial series of hydrodynamic tests are still being analyzed.
- b. <u>TV Camera</u> A zoom lens has been added to the TV camera inside the containment vessel. Electrical connections in the control room and a small motor on the camera makes it possible to operate the zoom system from the control room.
- c. Measurement of Water Channel Gaps in EBWR Core IA Fuel Elements Data previously reported show that the irradiated fuel in EBWR Core IA is subject to swelling above 600°C. Calculations of expected maximum fuel element temperatures with EBWR at 100 Mw show that temperatures exceeding 600°C may be obtained. It is therefore quite likely that swelling of some of the U-Nb-Zr alloy fuel plates will occur when the reactor is operated at 100 Mw. This situation, should it occur, would be undesirable because of the possibility of ultimately closing coolant channels completely in the elements with a resulting loss of coolant. Repeated measurements of representative water channel gaps after intervals of reactor operation should give some prior indication of dimensional change before complete closure of the gap occurs. With this in mind, a procedure has been established to measure selected water channel gaps in EBWR fuel elements without removing them from the reactor vessel.

An eddy current technique is applied in measuring the channel gap. A commercial unit, normally used for detecting flaws in materials, was modified for the present application. A special single wound coil probe was made and potted in a waterproof holder. Twenty feet of flexible cable is connected to the holder. This probe is mounted in a spring loaded positioner which positions the probe within a channel holding a constant probe-to-plate spacing on one face and measuring the variation of magnetic inductance as a function of the distance from the opposite plate face. The readings of the channel gap are recorded continuously.

The water channel gaps in EBWR fuel elements ET-15, ET-25, and ET-43 were recently measured. These elements were chosen because of their particular locations in the core, where highest fuel temperatures are expected. The channels ranged in thickness from 0.330 in. to greater than the reference value of 0.438 in.

The response of the measuring probe is temperature sensitive; consequently, the temperature within a channel was measured with a chromelalumel thermocouple before dimensional measurements were made. As there was no detectable gradient along a channel the probe was then calibrated at the measured temperature using a standard and go-no-go gauges. The standard consisted of two sections of unirradiated EBWR fuel plate that could be adjusted for known separation between the plates.

After calibration, the equipment was mounted on the indexing plug at a point above a positioning rack holding the EBWR fuel element to be examined. The probe holder was indexed over and driven into the channel to be measured. The signal from the probe, as it traversed a channel, was continuously recorded. Duplicate runs on some channels indicated that reproduction of the measurements was good. Relative variations along each channel were immediately apparent and actual water channel spacings were obtained by comparison of the chart values with those obtained from the known standard.

The estimated accuracy of the recorded values is  $\pm 0.010$  in. The variation in the values was more pronounced for the irradiated fuel elements than for unirradiated fuel elements. The scale deposits on the irradiated elements are considered to be responsible for the observed fluctuations in the measured values.

The charts will be retained and compared with similar charts made periodically throught the life of the Core I elements after additional burnup and elevated temperature operation is obtained.

#### C. BORAX-V

#### 1. Installation of Reactor and Components

The bottom faces of all the Al-Ni alloy boiling core hold-down boxes have been built up by weld overlay and remachined to make them flat and square and to assure uniform box length. Boiling fuel assemblies, dummy boiling fuel assemblies, hold-down boxes, chimneys, and control rod channel orifices have been successfully test-fitted in the boiling core structure. The spacers for the outside hold-down latches have been sized, machined, and installed. A mounting bracket for the magnetic, drag-disk-type downcomer flowmeter has been installed on the boiling core structure.

The reactor vessel, steam system, condensate system, feedwater system, auxiliary water and preheat systems, reactor water demineralizer system, superheater flood-and-drain system, forced-convection system, drains, traps, etc., have been given a hot detergent cleaning. Considerable quantities of rust, slag, metal filings, rocks and sand were removed from the

system by cleanup screens and filters. After the flushing operation some sand and slag were found on the bottom of the reactor vessel. The vessel has been washed out, as have the control-rod-drive nozzles and forced-convection nozzles. The reactor vessel wall is in good condition with only a few small surface rust spots evident. A thin layer of iron oxide remained on pipe interiors in some places.

Since the cleaning operation, the differential pressure probes, Staucheibe tube, and two reactor water sampling lines have been installed on the vessel wall in the downcomer region and the special flange and associated valves and piping for these items have been connected and installed on the southwest instrument nozzle. The saturated steam collector has been modified to give more clearance between it and the core structure and it has been refitted into the vessel. The control-rod-drive-nozzle shield plugs, control rod drives, seals and dash pot housings have been removed, cleaned and reinstalled.

Preparations have been made for a hydrotest and 600 psig, 489°F preoperational tests on the reactor vessel and internals, electric preheat, auxiliary water, reactor water demineralizer, feedwater, seal water, boron-addition and batch feed systems. The forced-convection system has been disconnected for high-temperature operation, and the forced-convection nozzles on the reactor vessel have been blanked off. The boiling core structure-Belleville spring assembly, feedwater sparger, saturated steam collector and superheated steam line caps have been installed in the reactor vessel. All process system filters have been loaded with fresh cartridges.

The defective Neva-clog filter plates found in the makeup water polishing demineralizer and the reactor water demineralizer have been replaced, and the tanks rewelded, hydrotested and reinstalled. Resin has been charged into the polishing, reactor water and condensate demineralizers and these items are ready for service.

Sampling lines for steam dome and reactor water samples have been run from the sampling station to the upper reactor pit. A high pressure, high temperature reactor water sampling pump has been placed in the subreactor room.

Installation of the revised seal water supply, return and control system for the forced-convection pump and the control and alarm wiring for this system has been completed. Installation of the boron-addition system pipe-heating tapes and controls is nearly complete.

The shield temperature alarm and indicator was remounted, calibrated, and the alarm point set. Alarm points were also set for reactor water demineralizer high temperature and condensate demineralizer high temperature.

The scram bypass circuits are being changed to add a high superheater-temperature-scram "Off" key switch.

Range changes were made on differential pressure cells for high and low reactor-water-level scram and low main-steam-flow scram to give more range for the former, and reduce the full scale range in the latter. Both changes were made to give better scram point accuracy.

The electric-to-pneumatic transducer on the superheater vent valve has been modified in conformance with design to open the valve on loss of normal electric power. A bypass switch circuit has been added to permit operation of the makeup water demineralizer supply valve independently of the makeup water storage tank level control system.

Revisions to the audio monitoring system are in progress to permit improved remote detection of forced-convection pump cavitation and excessive impact during control rod drops.

Recorders for all in-vessel instruments are mounted and most of the cable for these circuits has been pulled. Checkout of the control-rod drop timing circuit was completed.

#### 2. Procurement and Fabrication

a. Superheater Fuel - One hundred and ninety half-loaded, enriched fuel plates for the central superheater have been received from the vendor. Twenty-seven of these plates have been nondestructively tested and found to meet specifications with two exceptions. Ultrasonic and radiographic inspection indicates a non-bonded area on one plate. A surface rust spot was found on another plate. Chemical analyses of five samples from each of four destructively tested plates indicate that the maximum deviation in homogeneity of UO<sub>2</sub> distribution is \$\frac{1}{2}.92\%\$ of the average. Measurement of homogeneity by the gamma counting technique agrees very well with the chemical analysis method. Total U<sup>235</sup> content, as measured by gamma counting, is within specified deviations. The vendor has completed and shipped 154 fully-loaded enriched central superheater fuel plates.

To date five developmental 4-plate superheater fuel elements, using depleted  $\rm UO_2$  plates, have been brazed using Coast Metals 60 brazing alloy. Difficulty has been experienced with incomplete melting of the braze alloy due to poor temperature distribution in the small Glo-bar furnace used for this work. The brazed fuel elements, in general, appear to be satisfactory with the exception of an unexplained increase in width of the fuel element after brazing. Measurements of fuel plate width after brazing indicate no permanent plate growth. A test element using dummy fuel plates of Type 304 stainless steel showed no excessive width after brazing. Investigation of this problem is continuing.

system by cleanup screens and filters. After the flushing operation some sand and slag were found on the bottom of the reactor vessel. The vessel has been washed out, as have the control-rod-drive nozzles and forced-convection nozzles. The reactor vessel wall is in good condition with only a few small surface rust spots evident. A thin layer of iron oxide remained on pipe interiors in some places.

Since the cleaning operation, the differential pressure probes, Staucheibe tube, and two reactor water sampling lines have been installed on the vessel wall in the downcomer region and the special flange and associated valves and piping for these items have been connected and installed on the southwest instrument nozzle. The saturated steam collector has been modified to give more clearance between it and the core structure and it has been refitted into the vessel. The control-rod-drive-nozzle shield plugs, control rod drives, seals and dash pot housings have been removed, cleaned and reinstalled.

Preparations have been made for a hydrotest and 600 psig, 489°F preoperational tests on the reactor vessel and internals, electric preheat, auxiliary water, reactor water demineralizer, feedwater, seal water, boron-addition and batch feed systems. The forced-convection system has been disconnected for high-temperature operation, and the forced-convection nozzles on the reactor vessel have been blanked off. The boiling core structure-Belleville spring assembly, feedwater sparger, saturated steam collector and superheated steam line caps have been installed in the reactor vessel. All process system filters have been loaded with fresh cartridges.

The defective Neva-clog filter plates found in the makeup water polishing demineralizer and the reactor water demineralizer have been replaced, and the tanks rewelded, hydrotested and reinstalled. Resin has been charged into the polishing, reactor water and condensate demineralizers and these items are ready for service.

Sampling lines for steam dome and reactor water samples have been run from the sampling station to the upper reactor pit. A high pressure, high temperature reactor water sampling pump has been placed in the subreactor room.

Installation of the revised seal water supply, return and control system for the forced-convection pump and the control and alarm wiring for this system has been completed. Installation of the boron-addition system pipe-heating tapes and controls is nearly complete.

The shield temperature alarm and indicator was remounted, calibrated, and the alarm point set. Alarm points were also set for reactor water demineralizer high temperature and condensate demineralizer high temperature.

Drawings of the oscillating rod rotor assembly have been sent to the shop. Completion of the in-vessel drive shaft assembly design is being held up pending as-installed measurements on the core structure in the reactor vessel. Design of the oscillator rod drive continues.

Detailed design of the magnetic drag-disk-type flowmeter for measuring downcomer flow was completed. Detailed design continued on the fuel handling tool for reloading boiling fuel assemblies through the reactor vessel head nozzles. Detailed design was started on a boiling-fuel-rod gammascanning machine which will be used to determine boiler flux distributions during power operation, and on high pressure in-core thimbles to be used for irradiating flux wires and miniature counters under similar conditions. Detailed design was also started on special high efficiency plugs for the reactor top shield to be used with experiments in the reactor vessel head nozzles.

Due to the possible unavailability of AFSR, the BORAX-V exponential experiment, which is planned to check out the Cd-ratio technique of in-core void measurement, has been rescheduled for installation in the TREAT shield. The necessary design modifications to the already fabricated equipment for installation in TREAT have been made.

Analyses have been made of two additional accidents verbally posed by the ACRS. One of these accidents assumes a massive failure of the interpass plenum on the central superheater core allowing the superheater to flood rapidly in conjunction with a cold water accident. The second accident assumes the complete failure of a four plate superheater fuel element while venting steam to atmosphere at powers above 20 Mw.

#### 4. Development and Testing

a. Control Rods - Dye penetrant tests had previously indicated that there were surface defects in areas adjacent to some of the spot welds on the control rods. Radiographs and photomicrographs of these spotwelds have now shown that this defect is a circular ridge of metal pushed up by the weld. No cracks or porosity were found in the cladding, although some porosity in the spot weld nuggets was indicated. Two blades from a defective rod were cut off, seal-welded, and pressurized with gas to test the strength of the spot welds. The spot welds failed at internal pressures of from 250 to 350 psi, indicating that strength is adequate. Attempts to repair the porous nuggets by welding the outside of the stainless cladding at the spot weld was not effective. Radiographs of the edge and end welds of the cladding show that these welds are satisfactory.

As a result of these and previous tests, it has been decided that the 15 poison sections of control rods which passed the initial two week

autoclave test at 600 psig, 489°F conditions can safely be used for the initial operation with a boiling core. Eleven of these rods have been reautoclaved for 9 days as a final proof test. Results of this test are not yet available.

Development work on an improved, spot-welded joint continues. Improvement of dimple contours is being attempted. New control rods, using a new spot-welding technique will be fabricated for installation in the superheating cores.

b. <u>Corrosion Tests</u> - Type 304 stainless steel assemblies brazed with Coast Metals 60 alloy (nickel 20% - chromium 10% - silicon 3% and iron) and NIORA alloy (82% gold - 18% nickel) are being tested in superheated steam at 540°C and 650°C (600 psi in both cases). The joints appear in good condition after the following exposure time: Coast Metals 60 - 147 days at 540°C and 93 days at 650°C; NIORA - 109 days at 540°C and 93 days at 650°C.

Considerable flaking of oxide scale has occurred on the Type 304 stainless steel at 650°C. At 540°C a small void has become visible in two of the bonds of the Coast Metals braze samples. However, it appears that these voids became visible as a result of corrosion of smeared-over stainless steel produced during sample fabrication and are not the result of corrosive attack on the bond. Voids are not uncommon in the as-brazed samples.

Type 406 stainless steel continues to be much superior to Types 304, 316 and 347 after about 90 days at 650°C and 600 psi. Type 406 shows small weight gains. The 300 series materials are covered at least partially with spalling oxide.

The autoclave in which these samples are tested is also made of a 300 series stainless steel but exhibits no spalling. Two possible explanations have been advanced to explain the spalling on the small, thin samples and the lack of spalling on the autoclave. These are:

- Thin plates have a larger dimensional change when thermally cycled.
- The autoclave has a protective film built up during previous runs at lower temperatures.
- c. In-Core Instrumentation Development Four tantalum-sheathed samples of  $\overline{W/W}$ -26% Re boiling fuel rod thermocouples underwent tests to approximately 4600°F at Thermatest Laboratories of Sunnyvale, California.

Severe damage, some of which became evident at temperatures as low as 2200°F, resulted from this test. The sheath of one sample cracked near the tip, producing a slight shift in emf output at about 2200°F. All four samples, which were bound together by a tungsten wire, became solidly

fused at the end of the test. Severe flattening of the emf versus temperature curve occurred above 3800°F. These data showed a much lower emf above 3800°F than either Hoskins Mfg. Company's published data on bare wires, or data obtained in previous tests at Hoskins on similar samples from the same vendor. Performance up to about 3000°F matches quite well with earlier test data obtained at ANL.

The specimens have been examined by Laboratory personnel and it has been noted that extensive BeO-Ta reactions occurred, causing fusion of the samples. An additional reaction was noted between the Ta sheath and the tungsten binding wire.

Modified tests will be conducted on 4 additional samples as soon as they can be fitted into the work schedule of the testing laboratory. It is planned to limit the temperature to about 4000°F on these tests, and to check for moisture inside the sheaths, prior to testing. Moisture was a possible (though not probable) cause of the serious BeO-Ta reaction.

The Ta sheaths of 35 assembled thermocouples were inspected with the differential coil eddy current instrument. Defects in the sheath of 14 out of the 35 were indicated by the eddy current traces; however, metallographic examination of two pieces that were supplied for destructive evaluation revealed no internal defects in the sheath. The defects indicated were of the form of flat areas on the O.D. of the tubing. One such area that was sectioned showed that the outside of the tube was hexagonal while the I.D. was round. This indicates that the wall is thinner in the flat areas. External examination of the thermocouples that gave similar indications on their traces revealed that they have the same type of flat areas. However, only one of the 14 appeared to be as defective as the piece that was sectioned.

d. <u>Plant Tests</u> - During the process system cleaning operation, the feedwater flow controls and flowmeters, feed pumps, condensate pumps, auxiliary pump and electric preheaters were placed in operation. All checked out satisfactorily except that the feed pump motors overheat and the condensate pumps do not provide rated output. The feed pump motor problem has been referred to the vendor. The condensate pumps (holdovers from BORAX-III) are being investigated.

The continuous oxygen analyzer was checked and found to be flow-rate sensitive at values above 175 ml/min. This is above the intended flow rate, hence no trouble in use is anticipated. The analytical method for determination of  $\rm O_2$  dissolved in water has been set up and is in use.

Using a neutron source, plateaus have been run on the two  $BF_3$  proportional counter startup circuits. These circuits are satisfactory. All nuclear instrument ion chambers have been calibrated in AFSR and the linear,

safety, log power and period circuits have been checked out with a current source. The period trip circuits have been tested for spurious scrams due to electronic noise from the process system electrical equipment, control rod drive relays and motors, etc. At zero neutron flux noise is not a problem.

#### II. SODIUM COOLED REACTORS (040103)

#### A. General Research and Development

#### 1. ZPR-III Experiments

Work continued this month on the program related to the Fermi B reactor mockup, Assembly 35. Experiments to determine the effects of fuel heterogeneity were completed and measurements were made of reactivity coefficients of material in the core.

a. Fuel Heterogeneity Experiments - One of the major differences between the actual Fermi B core and the mockup lies in core fuel heterogeneity. The dispersion of  $UO_2$  in the Fermi cermet fuel plates gives a fairly homogeneous uranium composition, whereas in Assembly 35 the uranium is clustered in  $\frac{1}{8}$ -in. columns separated by about 2.4 in. of other materials. To evaluate the reactivity effect due to this difference of fuel arrangement, experiments with "bunching" and "unbunching" of uranium columns were performed.

In one experiment, forty  $\frac{1}{8}$ -in. columns of enriched uranium were bunched into twenty  $\frac{1}{4}$ -in. columns, resulting in a gain of 63.5 inhours. In another experiment, twenty  $\frac{1}{8}$ -in. enriched columns were reconstructed from double  $\frac{1}{16}$ -in. columns and then unbunched into forty separate  $\frac{1}{16}$ -in. columns with a total reactivity loss of 18.6 inhours. If the results are extended to the total core uranium content and extrapolated to zero-inch plate thickness, the worth of going from  $\frac{1}{8}$ -in. uranium plates to a homogeneous composition would be 620 inhours. The measured heterogeneity effect of the assembly is thus about -1.48% k.

b. <u>Distributed Reactivity Coefficients</u> - Measurements were made of the average worths in the core of all materials present in the core plus other materials of interest. In one half of the reactor, a distribution of 27 core drawers was chosen for a uniform core sampling. A series of substitutions of various materials was made in these drawers. Because of the distribution over half of the reactor, the net perturbations of material densities in the core were small. The materials substituted and the experimental results are given in Table II.

Table II. Core Average Reactivity Coefficients, Assembly 35

Material	Worth (ih/kg)
93% Enriched U	33.9
Depleted U (0.2% U <sup>235</sup> )	-1.2
$U^{235}$	36.5*
U <sup>238</sup>	-1.3*
Stainless Steel 304	2.2
Iron	1.9
Nickel	2.8
Sodium	13.7
Fe <sub>2</sub> O <sub>3</sub>	7.5
Oxygen	21.7
Physicums I & II** oxide	-2.6

<sup>\*</sup> Derived from fist two measurements

c. Radial Variation of Enriched U Worth - Measurements were made of the worths of enriched uranium columns at different radii from the core axis. These data are useful for the calculations of fuel rod bowing coefficients. In Table III, the distances from the core axis to the column center at which the worths were found are given along with the measured reactivity coefficients.

Table III. Enriched U Worth at Different Radii

Effective Radius,	Worth, (in	hours/kg)-Column
(in.)	l row nickel	2 row nickel blanket
0.03	61.8	
4.40	56.6	
8.67	45.2	
13.04	30.3	32.1
17.54	17.1	18.8

The effect of thickness of the nickel reflector bordering the core radial edge on the worth of an enriched U column was also measured. The Ni reflector around an angle of about  $\pi/6$  of the core in one-half the reactor was increased from one to two rows of Ni drawers. Near this double-row Ni, the worths of enriched U were remeasured at radii 13.04 and 17.54 in., the results are also shown in Table III.

<sup>\*\*</sup>A mixture of Ph I oxide and Ph II oxide was used for the determination. These materials are described in P/958 of the 1958 Geneva Conference on Peaceful Uses of Atomic Energy.

d. <u>Radial Variation of Sodium Worth</u> - Measurements were also made of the worths of sodium columns at different distances from the core axis. Empty steel cans were substituted for Na-filled cans in different radial zones. The average radii of the substitutions is given in Table IV, along with the results.

Table IV. Worth of Na in Columns at Different Radii

Column Lengths (in.)		ths	Average Radius (in.)	Worth, (inhours/kg)	
	18		1.72	18.8	
	18		6.53	17.4	
	18		13.11	14.5	
	18		17.71	9.4	
	21		19.42 (in Ni reflector)	5.7	

Variation of the thickness of nickel reflector was found to have no effect on the sodium worth near the core radial edge.

e. <u>Local Worths of Sodium in Core</u> - The reactivity coefficient of sodium was measured at nine localized positions in the core. These nine locations represent three axial positions (a. center, b. midway to edge, and c. edge) and three radial positions (I. center, II. midway to edge, III. edge). Table V contains the experimental results arranged according to positions of the measurements.

The general pattern of these reactivity coefficients confirms that predicted by PRDC calculations, the worth of Na being higher at the center, decreasing toward the axial and radial edges.

Table V. Local Reactivity Coefficients of Na in Core (inhours/kg)

		Radial Zone	
	I	п	III
Axial Region	0 to 3.3 in.	7.7 to 9.9 in.	16.5 to 18.7 in.
a. z* = 0. to 4 in.	19.9	18.6	12.8
b. $z = 7$ to 11 in.	19.2	14.4	10.5
c. $z = 14$ to 18 in.	15.2	9.3	5.9

<sup>\*(</sup>z = 0 is at core center)

Experiments are nearing completion measuring the variation of sodium worth as a function of sodium density in various regions.

#### 2. ZPR-III Analysis

Criticality calculations for the carbide ZPR-III assembly No. 34 were carried out. The core composition was 4.67 vol-%  $U^{235}$ , 10.35 vol-%  $U^{238}$ , 24.64 vol-% stainless steel, 25.46 vol-% aluminum, and 9.11 vol-% carbon. The 16-group cross-section set of Yiftah, et al., with his "conservative" values of  $\nu(U^{235})$ , was used. The aluminum and stainless steel transport and elastic removal cross sections, however, were those calculated by the ELMOE program. The aluminum cross sections were obtained from the analysis of the aluminum diluent assembly No. 23 and the stainless steel cross sections were obtained from the stainless steel diluent assembly No. 32. The SNG(S\_4) calculations on assembly No. 34 gave a reactivity excess of about 1.6%  $k_{\mbox{eff}}$  above that observed experimentally. This may be compared with the 4.6%  $k_{\mbox{eff}}$  obtained using the unmodified Yiftah set and standard  $\nu(U^{235})$  values.

#### 3. ZPR-VI

a.  $\frac{\text{Hazards Summary Report}}{\text{would be able to handle the high temperature gases associated}}$  with a uranium fire. A system incorporating the use of high temperature filters is being designed to meet this requirement. The Hazards Report is being revised to include the effects of using this venting system in conjunction with an argon purging system.

Calculations were made for peak pressures based on a heat generation rate after an initial energy release of  $10^7\,\mathrm{cal/min}$  for two proposed systems. The first of these utilizes the two existing 3-in. diameter pipe penetrations; the second would be a modification of the present 24-in. diameter ventilating system involving valving, filters, plenum, and atmospheric stack.

Discussion of the possible hazards associated with the use of plutonium are now being incorporated into the report.

- b. Bed and Table Assembly The movable and stationary tables have been put onto their respective positions on the beds. Final adjustments are being made with a load of about 90 tons of steel plate on each table. Tests to determine whether the bed and table assembly meet specifications are being made.
- c. Matrix Assembly About 93% of the square stainless steel tubes for the matrix have been received from the vendor. Bundling of the tubes into a 25-tube cluster is in a trial stage. A fixture to maintain the tubes in a square cluster prior to welding has been constructed and is being tested.

- d. <u>Control Console</u> The control console and instrumentation was inspected at the vendor's plant. The first console was complete except for the final wiring checkout. The second console is about 70% complete and should be ready in about four weeks.
- e. Miscellaneous Preparations  $BF_3$ -filled ionization chambers for the facilities were received from the vendor. These have been checked out with a source and with the ATSR facility. Two of the twelve chambers were found to be defective and are being returned to the vendor.

 $\,$  Two TV camera traverse assemblies have been inspected at the vendor's factory and accepted.

The enriched uranium for use on the two facilities is now being coated with a KEL-F coating with a red pigment. All of the depleted uranium has been coated.

A rough draft of the Operations Manual for the ZPR-VI has been completed and is being reviewed.

f. Experimental Preparation - A miniature  ${\rm Li}^6$ -coated counter has been constructed and tested with a Ra-Be neutron source. The multiplication has been improved increasing the signal-to-noise ratio. Tests are continuing in the ATSR facility.

A  $U^{236}$  miniature fission counter has been constructed and tested in ATSR. A small preamplifier is being designed to work with the counter inside of a tube of about  $\frac{1}{2}$ -in. diameter in ZPR-VI.

Specifications for a time analyzer for measuring the prompt periods of a reactor from 1 microsecond to a few milliseconds have been written. This analyzer will be used to measure the Rossi- $\alpha$  or prompt neutron periods in various assemblies in ZPR-VI.

g. Leak Test of Shielded Cells - Cell No. 5 was pressurized to 10 psig (2/3 atm) for a trial run. It was apparent after a short period that the rate of leakage via all paths was several orders of magnitude greater than the expected leakage rate. Measurement of leakage was abandoned in favor of an extensive survey for leaks.

#### B. EBR-I

#### 1. Fabrication of Core IV Fuel Elements

To provide 430 fuel rods plus fuel thermocouple rods, 521 jacket assemblies were completed in June, 1961, an excess of 21%. After inspection of the 521, and rejection of assemblies having excessive weld defects, an estimated 80 to 100 additional jacket assemblies must be completed.

Most of the acceptable tubes have been loaded and are now in the production process. Work has started on the X-ray recheck of all 321 previously loaded assemblies. The current radiographic rejection rate, while not excessive, has exhausted the limited supply of available tubing. A production run of tubing has been started, with a scheduled delivery date of December 1, 1961.

The production rate of finished elements may lag behind anticipated schedules because of the manpower burden resulting from the above outlined radiographic requirements. Six tangential X-rays of each element is now standard operating procedure.

#### C. EBR-II

#### 1. Reactor Operation - Dry Critical Experiments

The program as planned for the Dry Critical Experiment proceeded quite satisfactorily and was essentially completed at month's end.

Control rods were calibrated and it was found that their worths were in substantial agreement with predicted values. A special control rod containing boron-10 carbide was installed in place of a standard control rod and its worth was found to be about 70% greater than the standard rod in that position.

Table VI shows a comparison of measured and predicted values for control and safety rods.

Description	Measured % ∆k/k	Predicted % \( \Delta k \setminus k \)	
Control rod on "corner" of hex	0.33**	0.32	
Control rod on "flat" of hex	0.37**	0.32	
Special (B <sub>4</sub> <sup>10</sup> C) rod on corner of hex (rod 7)	0.56**	0.55 (<0.6)	
All twelve control rods	4.34†	3.84*	
Two safety rods	0.95†	1.1	

Table VI. Control and Safety Rod Worths

The worths of fuel subassemblies when substituted for blanket subassemblies at the corner and on a flat of the essentially hexagonal loading for the dry critical were measured and were found to be  $0.27\% \ \Delta \, k/k$  and  $0.38\% \ \Delta k/k$  respectively.

<sup>\*</sup>Shadowing effects (estimated at less than 10%) neglected.

<sup>\*\*</sup> Positive period calibration

<sup>†</sup>Subcritical multiplication measurement

A series of foil irradiations were performed in the blanket. The foils are being analyzed by radiochemical techniques and will give information on both power generation and neutron energy spectrum in the blanket.

A prototype oscillator rod was statically calibrated with poison loads of 71 grams and 129 grams of boron carbide ( $B_4^{10}\,C$ ). The measurement was repeated with the poison replaced by a low density aluminum spacer in order to isolate the effect of the poison. The experiments indicate that a poison loading in this range will give satisfactory  $\Delta k/k$  amplitudes for oscillator studies, with dk/ds almost constant over a 3-inch stroke.

An isothermal temperature coefficient experiment was performed as part of the Dry Critical Experiment. This was accomplished by first cooling the reactor, using temporary ducts from the building supply air system to direct cold air down into the primary tank through empty nozzles in the cover. A circulation system within the primary tank was used to circulate the cold air in the primary tank and through the reactor core. After the reactor core reached a temperature of about 58°F, a critical run was made to determine reactivity of the cold core.

The cooling was then stopped and the primary tank immersion heaters were turned on intermittently (connected to give about 75 kw total output) to warm the reactor. (The circulation system in the primary tank was again used to circulate the warm air.) When the reactor reached a temperature of about 99°F, a critical run was again made. These runs give a preliminary value for the temperature coefficient of reactivity of -2.5 x  $10^{-5} \, \Delta \, k/k^{\circ} \, C$ .

During the course of the experiment, rod worth measurements were made, as convenient, for various locations by switching fuel and blanket elements in these locations.

#### 2. Sodium Boiler Plant

a. Cleaning and Inspection - All chrome-moly pipe welds, except those affiliated with the superheaters and the evaporator which is in Illinois for repair, have been completed, X-rayed and stress relieved. This constitutes approximately 70% of the pipe welding which was to be accomplished. Verification of the pipe material and weldment, and a test of a weldment hardness has been completed by Laboratory personnel. Magnetic ferrite tests on stainlesss steel weldments made by the Package III Contractor have also been performed. This investigation revealed three chrome-moly welds of unacceptable hardness and a few stainless welds with borderline ferrite content. The remainder of the material appeared substantially satisfactory.

Progress on corrective work is 65% complete, punch items are about 15% complete and the originally scheduled work is about 30% complete.

b. Leak Testing of the Evaporator - Evaporator No. B3-EV702 is now at the Laboratory for repair. Both the shell side and the tube side of the unit were given a helium mass spectrometer leak test. The tube (steam) side was helium leak tight as measured with a mass spectrometer having a sensitivity of  $10^{-10}$  atm cc/sec/scale division. The leak in the shell (sodium) side as determined at the site and reported in the Progress Report for August 1961 (ANL-6409) was confirmed.

The unit was also helium leak tested with the tubes in tension. During fabrication the tubes were cold sprung approximately two-thirds the amount of design strain. This placed the tubes into compression. During operation a temperature difference exists between the shell and the tubes, with the shell being at the higher temperature. This temperature difference relieves the compressive stresses in the tubes and at design conditions imposes a small tensile strain.

A helium leak test was conducted with a temperature difference imposed on the unit such that a tensile strain slightly in excess of the compressive strain produced by cold springing was imposed on the tubes. The leak rate measured under these conditions did not increase.

Leak testing of the "as-received" unit is complete and removal of the steam head and tube sheet is in process.

#### 3. Power Plant

The installation of drains and vents in the condensate system has been completed and the condensate storage tank, hot well and No. 2 feedwater heater controls are operating.

A supply of gland sealing steam from the auxiliary boiler has been piped to the turbine. The cooling tower fans have been operated and the time delays on their controls have been set. Installation of the initial pressure governor transfer relays completed the electrical wiring for the turbine. With the shaft sealing system of the turbine including the pump operable, the system is now ready to have a vacuum applied to the condenser.

#### 4. Instrumentation and Controls

a. <u>Nuclear Instrumentation</u> - The nuclear instrumentation for the EBR-II Dry Critical Experiments has performed satisfactorily. The largest of the "debugging" problems encountered was in the interconnection cabling and was due to multiple grounding points and wiring errors.

The major equipment problem occurred in the in-core instrumentation installed temporarily for this experiment. Commercial linear pulse amplifiers, which operated satisfactorily during tests, failed when operated

continuously. These were replaced with ANL-designed amplifiers, of the type used in the normal EBR-II operating instrumentation and reliable operation was obtained. All major problems were corrected before the reactor loading began and no significant instrumentation problems arose during the critical approach or during subsequent critical experiments.

The results of the Dry Critical Experiment flux measurements indicate that in-core instrumentation will not be required for wet critical loading, if two high sensitivity proportional counters are empoyed in the normal instrument thimbles. These detectors would feed the two counting rate channels previously used for in-core instrumentation. The addition of this instrumentation will make no change in the regular operating channels. These counters will be installed prior to the Dry Critical unloading operation and tested for sensitivity and response as the reactor is unloaded.

b. Fuel Handling Center - During October the system has been used for occasional transfers of the neutron source, etc., incidental to the Dry Critical Experiments. After these experiments are completed, the enriched subassemblies will be unloaded from the core and inner blanket.

Final drawings and tracings for the fuel handling system have all been received from Datex. Minor revisions are now being made on the tracings to incorporate ANL changes to the equipment.

The wiring of the refueling machine is near completion at Argonne, Illinois. It is expected that the machine will be ready for test on November 8.

#### 5. Component Development - Steam Generators

The tube-to-sodium tube sheet welds have been made on the second modified evaporator (which will be used as a superheater). The steam tube sheets are being installed. The major difficulty, the tube-to-sodium tube sheet welds, which has been delaying fabrication, has now been overcome.

#### 6. Component Development - Fuel Reprocessing Facilities

a. Fuel Cycle Facility - The Fuel Cycle Facility is slightly more than 96 percent complete. Progress has been very slow during the past few months; however, the contractor is increasing his work force and an improvement in construction activity is anticipated.

Checking of heating, ventilating equipment and controls is continuing. Electrical tie-in work is being done on contractor-supplied instrument panelboards. The panels, however, require a considerable amount of corrective work to bring them up to specifications. This work is now underway.

Reworking of the window shutter, crane, and manipulator rails in the Argon Cell has been started by the subcontractor in order to bring the rails up to contractual specifications.

Operational load tests were made on the 20-ton high-bay bridge crane and on the 20-ton passageway hoist for lifting the interbuilding coffin. The crane and hoist failed to meet specifications and corrective measures are now being undertaken.

Work is continuing on equipment for the Fuel Cycle Facility. New drawings of the interbuilding coffin, which will be used to transport fuel elements between the reactor and the Fuel Cycle Facility, were received, reviewed and rejected because they again did not meet design specifications. Fabrication of the melt refining furnaces has been completed. The control panels for the furnaces have been received in Idaho. Tests revealed that corrective work will be required before the panels meet specifications. The window shutters have been completed and shipped to Idaho.

The collapsible stand for holding manipulator carriages has been tested in the mock-up. The stand has now been shipped to Idaho.

As a result of favorable experience with a magnetic clutch (manufactured by Lear, Inc.) in the prototype manipulator, the grip drives of the operating manipulators for the Argon Cell will be equipped with this clutch.

Three runs were made to investigate the sorption of magnesium-zinc vapors by molded Fiberfrax fume traps. Fifty weight percent magnesium-zinc melts were distilled in the melt refining furnace and the distillates were collected on degassed standard Fiberfrax traps. With a 180-gram charge, the largest charge used in the runs, 91 percent of the charge was sorbed by the trap, and 7 percent was retained by the crucible assembly. Similar results were obtained in the runs with the smaller charges. Since the Fiberfrax trap did not appear to be saturated in the experiment with the 180-gram charge, additional runs will be made with larger charges.

b. Development of Remotely Controlled Methods and Equipment for Fuel Fabrication - The process equipment design work for EBR-II FCF refabrication equipment is 95% complete. Installation drawings and instructions are about 65% complete.

All nickel-plated parts for the injection casting furnaces (see Progress Report, September 1961, ANL-6433) have been received and the remaining ceramic parts are expected in November. The internal wiring work on the furnaces has been started.

Tests have been completed on the leak detectors and shipment to the Laboratory is scheduled for October 25, 1961.

The valve cabinets have been shippped to Idaho and the related subcell installation drawings and instructions are being prepared for shipment.

#### 7. Process Development

a. Melt Refining Process Technology - Additional work has been completed on the effect of nitridation of unirradiated EBR-II prototype pins on melt refining yields. The pins were exposed for two hours at 350°C to argon atmospheres containing from 0 to 5 percent nitrogen. The melt refining yields were unaffected by these exposures and ranged from 95.2 to 96.2 percent.

Apparatus for the determination of nitridation and oxidation rates of irradiated fuel pins has been installed and tested in the Senior Cave.

A mathematical treatment of data reported earlier (see Progress Report, April, 1961, ANL-6355) on the evolution of fission product xenon-133 from highly irradiated EBR-II-type fuel alloy suggests that the mechanism of fission gas release on heating involves microcracks and/or interconnected pores which serve as escape paths.

b. <u>Skull Reclamation Process</u> - Further studies have confirmed earlier data (ANL-6355) which show that a minimum critical concentration of magnesium ion in alkali chloride-magnesium chloride-magnesium fluoride fluxes is essential for the complete reduction of uranium and thorium oxides by zinc-magnesium alloy. The same effect is observed in calcium chloride-magnesium chloride-magnesium fluoride fluxes. The minimum critical concentration of magnesium ion needed for complete reduction appears to depend upon the conditions employed for the reduction.

Equipment for future demonstration runs of the skull reclamation process is to be installed in a large drybox which is now being prepared for this purpose. Demonstration of the skull reclamation process in a dry inert atmosphere will eliminate problems of corrosion associated with the hygroscopicity of the fused salt fluxes and of handling the pyrophoric retorted uranium product.

A demonstration run of the skull reclamation process was completed in which a beryllia crucible was employed for the last three steps of the process, namely, two uranium precipitations and retorting. About 85 percent of the uranium charged was recovered after retorting. Nine percent of the uranium remained behind as a recoverable heel in the crucible used in the reduction step.

An isostatically pressed beryllia crucible (4-in. OD by 9 in. high) which had been used in five runs, each including the last three process steps, developed hairline cracks on the sixth use. Hairline cracks also developed on the first use of a beryllia crucible fabricated from beryllia of finer grain. In both runs more than 99 percent of the product was easily removed from the crucibles. The development of the hairline cracks is attributed to low density areas within the crucibles. The manufacturer of the crucibles, the Brush Beryllium Company, is cooperating on the evaluation and manufacture of various types of beryllia crucibles to overcome the cracking problem. A flame-sprayed-and-sintered tungsten crucible is also being tested for the retorting operation.

- c. Blanket Processing A third successful demonstration run of the blanket process has been completed. In this run sodium was added to give a concentration which may be expected from the dissolution of sodium-coated EBR-II blanket rods. No adverse effect of the sodium on plutonium recovery or separation from uranium was apparent. Ninety-three percent of the plutonium was isolated in magnesium-rich supernatant solutions. Material balances for both uranium and plutonium slightly exceeded 100 percent.
- d. Fused Salt Studies In order to identify the uranium species present in the molten salt phase when uranium oxides are reduced to the metal by zinc-magnesium alloy, spectra of uranium compounds in salt systems of process interest are being obtained. A determination of the uranium trichloride spectra from 700 to 1300 m $\mu$  in equimolar lithium chloridemagnesium chloride at 635° and 730°C show a close resemblance to the curve obtained by Gruen and McBeth for uranium trichloride dissolved in lithium chloride-potassium chloride eutectic.
- e. Materials and Equipment Evaluation Materials evaluation studies are in progress to evaluate the compatibility of various materials with liquid metal and fused salt systems of the types contemplated for reprocessing reactor fuels. A flame-sprayed-and-sintered tungsten crucible has been used for a total of 237 hours at temperatures of 800° to 850°C in operations simulating those of noble metal extraction (extraction of noble metals into molten zinc from a slurry of skull oxides in a molten chloride flux) and skull oxide reduction (reduction of uranium oxides by magnesium in a zinc solution in the presence of a molten chloride flux). No sign of corrosion of the crucible is evident.

Specimens of a molybdenum-30 percent tungsten alloy exposed for 100 hours at 850°C to zinc, zinc-5 percent magnesium, and zinc-50 percent magnesium systems showed no observable signs of corrosion. This is a new alloy which is presently in the development stage. Fabrication technology for this alloy is still undeveloped. However, the alloy possesses some ductility at room temperature and may be more easily fabricable than

tungsten. Boron nitride was found to be excessively attacked at 850°C by zinc-magnesium systems. A tantalum-10 percent tungsten alloy is being evaluated as a material for corrosion capsules. A small graphite crucible in which tungsten was vapor-deposited on interior walls has been subjected to temperature cycling tests and to a zinc-magnesium solution containment test at 700°C. Metallographic examination after sectioning showed a slight separation of tungsten from the graphite at the line of cutting. It is not known whether this separation resulted from the test procedures or whether the separation occurred during the preparation of the sample for metallographic study.

Additional data were obtained on the corrosion of 405 stainless steel by cadmium-magnesium-zinc systems. The results substantiate previous conclusions that corrosion of 405 stainless steel is accelerated as the atom concentration of zinc increases. Variations in cadmium and magnesium concentrations were shown to have a lesser effect on corrosion, but a decrease in the cadmium concentration was found to reduce corrosion.

#### 8. Fuel Development - Core II

a. Fast Reactor Fuel Jacket Development - The desired higher operating temperatures for liquid metal cooled fast flux reactors and the use of plutonium alloys or other fuels which are not compatible with stainless steel at desired reactor operating temperatures require the development of new high-strength alloys for jacketing material. Most development work to date has been limited to available vanadium, niobium, and tantalum base alloys.

Initial attempts to anneal a Nb-4 w/o V-10 w/o Ti alloy strip by resistance heating were unsuccessful. The strip, while clamped between water cooled copper blocks, is heated by its own resistance when passing low voltage current through it in vacuo. After annealing at  $1400\,^{\circ}\mathrm{C}$  for 0.5 hours, the annealed portion of the strip was very brittle. Suspecting that gaseous contamination was responsible for the brittleness, samples of the annealed and unannealed material were submitted for analysis. Only the nitrogen analysis has been completed thus far and the results show an increase of 59% nitrogen in the annealed material.

b. Irradiation of Refractory Clad U-20 w/o Pu-10 w/o Fs Alloy - A group of 18 U-20 w/o Pu-10 w/o Fs alloy pins clad with various refractory metals is being examined in the hot cells. The specimens are prototype EBR-II fuel elements, in that the dimensions of the cladding and the sodium bond between fuel and cladding are identical to EBR-II design. The fuel diameter before irradiation was 0.144 in., the sodium annulus thickness 0.006 in., and the cladding tube wall thickness was 0.009 in. The overall length of each specimen was 3 in., or approximately one-sixth the length of a full size EBR-II fuel element.

The specimens had been irradiated in NaK or sodium filled capsules in CP-5 to burnups estimated to range from 1.0 to 1.5~a/o. The irradiation temperatures for most of the specimens were higher than the desired  $650^\circ$  to  $700^\circ$ C because of unexpectedly high fission rates resulting from spectral hardening in the fuel thimbles. As a result, all but three of the specimens were damaged to various degrees by overheating. In some cases the measured fuel temperatures approached  $1000^\circ$ C, well above the fuel alloy melting point of  $820^\circ$ C.

The preliminary evaluation of the condition of the specimens by autoradiographic techniques, described in the August, 1961, Progress Report (ANL-6409), has been confirmed by direct examination of the specimens in a hot cell modified for irradiated plutonium. For those specimens in which fuel melting occurred, vanadium appeared to be superior to the other cladding materials (niobium, Nb-1 w/o Zr alloy, Inconel-X, and 304 stainless steel). Under melting conditions the Inconel-X and stainless steel were the worst, as might be expected from their tendency to form eutectic with the fuel. A vanadium barrier foil 0.0005 in. thick has been wrapped around the fuel pin in all specimens with Inconel-X or stainless steel to prevent eutectic formation at the desired operating temperature.

The three specimens which did not fail were irradiated in the temperature range of interest (650° to 700°C) and these were found to be in good to excellent condition after the test. The cladding materials included vanadium, Nb-1 w/o Zr alloy, and 304 stainless steel. The diameter changes ranged from minus 0.0005 in. to plus 0.0021 in., or a maximum change of 1.2%. The vanadium clad specimen was slightly bent, whereas the stainless steel and Nb-1 w/o Zr clad specimens retained their original straightness. The vanadium clad specimen shortened 0.021 in. (0.06%), whereas length changes in the other two specimens were 0.001 in. (0.003%) or less.

The three specimens described above give some encouragement that the pronounced swelling tendency of the U-20 w/o Pu-10 w/o Fs alloy can be restrained by cladding of design thickness (0.009 in.) at EBR-II operating temperatures and burnups. Additional examinations to be made on the irradiated specimens include burnup analyses and metallographic observations of fuel-clad reactions. Irradiations will continue using other promising cladding materials as they are procured.

#### III. REACTOR SAFETY (040117)

#### A. Thermal Reactor Safety Studies

#### 1. Fuel-Coolant Chemical Reactions

Knowledge of the nature and extent of chemical reactions with nuclear reactor core metals that may occur in pressurized water or steam is essential to safe operation of reactors. The principal laboratory procedure uses a condenser discharge to provide almost instantaneous heating and melting of metal wire in water or steam. The energy input to the wire indicates reaction temperature; the transient pressure measures reaction rate; light emission indicates time-temperature; hydrogen generated gives extent of reaction; and particle size of the residue indicates the surface area exposed to reaction. A second method consists of heating the metal inductively and subjecting it to a steam pulse to induce a metal-steam reaction.

Studies of the kinetics of metal-water reactions under reactor incident conditions are being made in the TREAT reactor.

The series of condenser discharge runs with Zircaloy-3 wires in water was completed. A series of runs in heated water and a series in room temperature water showed good agreement with previous results with pure zirconium wires under similar conditions. Several additional runs were made to test the effect of added inert gas on the reaction of zirconium with heated water. Results indicate that there is no effect.

Data obtained on the reaction of molten aluminum with steam by the pressure-pulse method were re-examined and it was concluded that the reaction at 800°, 1000°, and 1200°C can be described by the cubic rate law. The reaction was found to have an activiation energy of 21.7 kcal/mole. Preliminary results with aluminum - 5 percent uranium alloys indicate that reaction is somewhat slower than with pure aluminum. Studies of reaction with aluminum - 20 percent uranium are underway.

The fourteenth series of metal-water experiments was conducted in TREAT. The purpose of this series was to determine the accuracy of fission energy input measurements. Uranium foils enclosed in each autoclave served as flux monitors. In addition, one of the autoclaves was modified so that a fission counter could be placed inside. Data from this counter indicated that about 3 fissions/ $\mu g \ U^{235}$  occur per watt-sec of reactor power inside the autoclave.

#### 2. Metal Oxidation and Ignition Studies

Studies are being made of the oxidation and ignition kinetics of the metals uranium, zirconium, and plutonium in order to provide information leading to an understanding of the reactions. This knowledge should make

it possible to minimize the hazards associated with handling these nuclear reactor materials. Isothermal oxidation on microscope stage, shielded ignition, burning curves, rate of propagation of burning foil, and burning temperatures are the techniques being used. In the continuing study of ignition and burning of uranium, zirconium, and plutonium, more emphasis is being placed on the burning process. Burning propagation rate studies provide a useful tool to observe the effects of many variables. The effect of the presence of halogenated hydrocarbons on the burning of uranium foil in air is being investigated.

Theoretical studies to relate isothermal oxidation rates to observed ignition behavior are continuing. Data for isothermal oxidation rates of Argonne Base and Battelle Base uranium in the heat sink apparatus were extended to include the temperature range from 300° to 600°C (previous data were obtained from 300° to 500°C). The oxidation rate with Argonne Base metal ( $\beta$ -quenched) decreased with temperature in the range 400° to 500°C indicating a change of mechanism. Rates with Battelle Base metal ("as cast") also indicated a changing character in this temperature range, however, the rates did not decrease with temperature.

Additional experimental studies of the ignition of zirconium were made in an effort to account for deviations from theoretical behavior. It was discovered that exposed ends of wire specimens could lower ignition temperatures significantly with samples of low specific area. Ignition occurred at the exposed ends and rapidly propagated across the specimen. When the experiments were performed using larger wires with ends shielded by "heat sink" caps, ignition occurred at higher temperatures and was initiated more uniformly over the specimen. The revised experimental results agreed more closely with theoretical predictions.

Halogenated hydrocarbons added to air have been found to lower the burning temperature of uranium and zirconium foils. From a systematic study of the effect of varying constitution of the hydrocarbons it has been found that (a) increasing chlorination increases effectiveness, (b) iodides are relatively ineffective, (c) the presence of a hydrogen atom is beneficial, (d) fully fluorinated compounds are relatively ineffective for uranium. They are somewhat effective, however, for zirconium which burns at a higher temperature.

Specific area measurements of irregular uranium monocarbide powders were made by a gas absorption method. Previously reported ignition temperature-specific area results were modified accordingly. The new results indicate a more consistent variation of ignition temperature with specific area for powders from different sources.

# B. Fast Reactor Safety Studies

## 1. TREAT Program

a. <u>Capsule Experiments</u> - The uranium oxide samples from Meltdown Series XXV were examined during this period. Samples 1 and 2 were clad in stainless steel; 3 and 4 were clad in tantalum. The conditions to which these samples were exposed in TREAT were listed in the previous Progress Report (ANL-6433). The pins were composed of 90% theoretical density material with an enrichment of 10.9%.

Although the maximum recorded cladding temperatures were 1260°C and 1800°C for steel and tantalum, respectively, no evidence of cladding failure was found in any of the specimens. The spacer wires on the first two samples produced extensive warping of the elements with consequent local fragmentation of the oxide. Samples 3 and 4 did not show the degree of fracturing seen in samples 1 and 2. It is reasonable to conclude that this was caused by the mechanical effect of the distortion produced. However, in sample 4 evidence was observed indicating that a definite oxide change occurred. The change took place along the central axis of the oxide cylinders and in many cases large cracks radiated from the center of the slug, with some running the entire length.

Series XXVI, the first experiments in the transparent facility with axially-shaped neutron flux at the sample, was successfully completed in TREAT during October. The film taken during the tests has been returned from Idaho and is being processed.

Preparations are being made for the first transparent experiments with argon-bonded uranium oxide fuel, clad in stainless steel and in tantalum. The considerably higher heat content of the fuel at failure requires some modification of the test facility to assure no melt-through of the sample capsules.

b. Package Sodium Loop - The first model of the package sodium loop was operated for several weeks at an approximate flow rate of 3.96 m/sec (13.0 ft/sec) at the operating temperature of 500°C. Following this, the power to the pump was raised to increase the flow rate to approximately 6.40 m/sec (21.0 ft/sec). During this time the temperature of the transformer and the sodium was followed to see what the increase of power would do. In an interval of 33 min the sodium temperature rose from 500°C to 595°C and the transformer from 176°C to 246°C. At the end of the time the flow failed. Subsequent examination showed that a portion of the pump coil had fused and that the transformer had shorted. However, the test showed that the equipment can function sufficiently long to allow experiments to be performed in TREAT without overheating or damage to the system.

The second loop is nearing completion with certain modifications incorporated to permit the exposure of thermite test elements in the loop in a laboratory experiment. This test will simulate the energy release expected during a TREAT experiment and will demonstrate loop integrity.

c. <u>Large TREAT Loop</u> - The heating power of the loop is to be 80 kw. A demister-molecular sieve combination has been specified in the tank interconnection line.

Experimental equipment has been erected for the testing of a Conoseal flange connection under exposure to a pressure pulse in a sodium system. A furnace is used to preheat a mass of metal balls to the vicinity of 1000°C. These preheated balls will then be dropped into a pool of sodium in the flange region. The duration of the pressure pulse and its magnitude will be measured. This test will give a quantitative indication of the ability of the flange to withstand a sudden pressure surge.

d. Remote Fuel Encapsulation - Tests were performed utilizing a technique developed for the final sealing of TREAT capsules. The method consists of inserting a wire plug with a small amount of silver solder into the pumpout tube of the capsule. When the insertion is completed, a portion of the tube is heated by passing a current through the tube. This produces a final seal when the silver solder melts and bridges the opening. The method appears to be fully satisfactory for effecting the closure.

#### IV. NUCLEAR TECHNOLOGY AND GENERAL SUPPORT (040400)

#### A. Applied Nuclear Physics

#### 1. High Conversion Critical Experiment

Measurements of clean configurations with BORAX-V fuel were continued. Three critical cores were assembled during October.  $UO_2$  fuel (4.95 wt-% enriched) in stainless steel jackets was used in each core. The lattice spacing used was 1.27 cm; both square and triangular lattices were investigated. The keff for cores completely submerged in water was measured for a number of core diameters. Values for the ICR and the ratio  $\rho$  = (capture cadmium ratio - 1) in  $U^{238}$  in the center of the square lattices were found to be  $\rho$  = 5.495; ICR = 0.555. From these data the resonance escape probability in  $U^{238}$  was calculated to be 0.623. Foil traverse data in conjunction with the point measurements in the core center are utilized to yield integral values of the parameters (averaged over the entire core).

A number of axial flux traverses have been fitted to the function

$$C \cos B_1(x - x_0) + D \cosh B_2(x - x_0)$$
 ,

where the values of C and D may differ for each traverse, while  $B_1$ ,  $B_2$ , and  $x_0$  are assumed to remain common to all. Six traverses were used, including bare and cadmium-covered uranium, dysprosium, and gold foils. The fit obtained had a chi-square very much larger than could be attributed to chance, so that the assumption that  $B_1$  and  $B_2$  could be considered the same for all traverses appears invalid.

# 2. Fast Spectrum Measurements

Solid state counters have been examined for their response to alpha particles produced in the boron  $(n,\alpha)$  reaction. Collimated particles reaching the detector surface in a vacuum were in one main energy group characteristic of the reaction that forms the excited state of the resulting lithium. A weak line characteristic of the reaction to the lithium ground state was also found. A resolution of the main line of about 10% was obtained. The line, when produced with collimated  $\alpha$  particles, showed suggestions of a fine structure when seen in a two-hundred channel analyzer. Since this fine structure appeared to be reproducible, a repeat experiment is being prepared to re-examine the line shape in greater detail.

Circuitry and instrumentation for the study of pulse rise times in a gas-filled counter are being constructed. A circuit which develops an output pulse of height proportional to the peak height ratios of coincident input pulses has been tested.

A neutron converter facility, designed to produce a spectrum roughly similar to that of a fast assembly, has been set up in front of one of the faces of the ATSR. The shielding sides remain to be completed.

# 3. Argonne Thermal Source Reactor

The thermostatically controlled immersion heaters which were installed in the storage and shield tanks of the ATSR have been set to keep the water temperatures at 34.0  $\pm$  0.3°C. With the aid of an auxiliary strip heater for fine temperature adjustments, it has been possible to reduce the reactor drift rate to 6.9 x 10 $^{-7}$   $\Delta k/k/hr$  approximately one hour after achieving criticality.

New control rods for the ATSR have been calibrated. An accurate plot of the reactivity change as a function of sample position in the central tube has been obtained. From this data, the stop in the sample tube has been adjusted so as to oscillate the sample in the region of maximum sensitivity to absorption effects and minimum sensitivity to sample scattering effects.

The final check of the detecting system has begun and noise data for one detector efficiency have been taken. Preliminary calculations indicate that the reactor power level will be between 60 and 100 watts.

## 4. Mathematical Numerical Methods Analysis

The general recursive algorithm for rational interpolation gives values of the constants  $\mathbf{a}_i$  in the interpolating function

$$\bar{f}(x) = a_0 + \underbrace{\psi_0(x)}_{a_1 + \underbrace{\psi_1(x)}_{a_2 + \cdots}}$$

which takes on specified values at  $x = x_j$  (j = 0,1,...n).

For  $\psi_j=x-x_j$ ,  $\overline{f}(x)$  can be reduced to the ratio of two polynomials. The algorithm places no restrictions on the form of  $\psi_j(x)$ , other than requiring that  $\psi_j(x_j)=0$ , and  $\psi_j(x_k)\neq 0$   $(k\neq j)$ . A wide range of types of interpolating functions are therefore open to experimental computation.

A program has been written to facilitate carrying out such computations on the LGP-30. For  $\psi_j(x)=\sin \Pi \ (x-x_j), \ \bar{f}(x)$  can be reduced to the ratio of two trigonometric polynomials. Using this interpolating function, the function f(x)=x was approximated by interpolation with  $x=1,\frac{1}{2},\frac{1}{3},\frac{3}{4},$  and  $\frac{1}{5},$  as base points. The maximum errors in the intervals between the various base points were determined using first only the first three points than the first four points and finally all five. (See Table VII below.)

Table VII. Maximum Errors for Various
Approximations

	Maxii	Maximum of $ \bar{f}(x)-x $		
Range	3 pt	4 pt	5 pt	
$\frac{1}{5 \le x \cdot 1/3}$	0.1211	0.0301	0.0035	
$1/3 \le \times 1/2$	0.0070	0.0003	0.0011	
$1/2 \le \times 3/4$	0.0137	0.0003	0.0011	
$3/4 \le x \le 1$	0.0124	0.0007	0.0012	

It is to be emphasized that these are results of a first numerical experiment. They indicate the validity of the algorithm, and the desirability of further study to determine more profitable functions for investigation.

#### 5. Theoretical Reactor Physics

a. Errors in Critical Experiment Doppler Coefficient Measurements - In very large fast reactors, particularly in those with oxide or carbide fuels, a significant part of the flux is in the neutron energy range 300-10,000 ev. It has been shown that because of this there is a Doppler temperature coefficient of the reactor which is probably large enough to be important for reactor safety. Calculations of this effect become quite simple if one assumes that resonances of fertile and fissile material are represented by the one-level formula and are well separated. This assumption is probably reasonably good for these low energy neutrons.

It may further be assumed that the narrow resonance approximation may be made and that interference between resonance and potential scattering may be neglected.

The capture or fission rate for each resonance then becomes proportional to an integral

$$J = \int_0^\infty \frac{\psi(x,t)}{\psi(x,t) + \beta} dx$$

 $\psi$  is a function which describes the Doppler broadened cross-section and has been tabulated.\* The parameter t is proportional to the absolute temperature of the reacting atoms.  $\psi$  appears in the numerator because the reaction rate is proportional to the reaction cross section. The  $\psi$  function in the denominator represents the perturbation in flux caused by variation in total cross section of the reacting atom. It is this perturbation

<sup>\*</sup>Rose, M. E., et al., WAPD-SR-506 (1954).

which is responsible for the Doppler effect, since  $\int_0^\infty \psi(x,t) dx$  is independent of t. Thus one can compute the error in Doppler coefficient measurement made with a small heated sample in a cold critical assembly by evaluating the  $\psi$  function in the numerator at the sample temperature and that in the denominator at the reactor temperature.

This process has been carried out for a few representative values of neutron and fission widths, though not for enough to obtain a proper statistical average. The indication from these first results is that the critical experiment measurement of  $\rm U^{238}$  Doppler coefficient is likely to be 50% of that with sample and reactor at the same temperature, and that the critical experiment measurement of the  $\rm Pu^{239}$  coefficient may be only about half of this value.

The conclusion to be drawn from this is that such measurements must be interpreted with care. These experiments will need to be carried out over a wide range of compositions and temperatures to be certain that the theory and parameters are well understood before applying the results to power reactors.

$$\beta_{\text{eff}}/\beta = 1.66$$

Assuming  $\beta = 0.0064$ ,  $\beta_{eff} = 0.0075$ .

For a critical bare reactor with the same core properties the effective delayed neutron fraction by age theory is 0.0087, and by a two-group analysis 0.0080.

c. Study of Shape Factors in Fast Reactors - Two dimensional Shape Factor Analyses (page 39, ANL-6409, Progress Report, August, 1961) have been treated by purely one-dimensional methods. It has been found that, in general, the simpler and less expensive one-dimensional methods are adequate for predicting all but the most detailed geometric effects.

Gold and indium studies were made to investigate self-shielding effects. They indicate that these effects are very large for the commonly used one mil foils and become small only for foils appreciably less than one mil thick.

- d. Fast Reactor Excursion Analyses The AX-1 Code, for study of severe reactor accidents, has been revised in some important ways. The equation of state, which relates the regional pressure to the local temperature and density has been altered to provide two new options. One new option allows for use of the Mie-Gruneisen equation of state which is based on an harmonic oscillator model of the solid and whose usefulness has been a subject of considerable study.\* A second option now available allows the material of any given region to turn to a Van der Waals type gas under proper conditions. This last option should be particularly useful in the study of severe accidents on experimental zero power assemblies. Other improvements in the code consist of allowances for more regions and materials.
- e. Resonance Integral Computations—The resolved resonance integrals for U<sup>238</sup>, Th<sup>232</sup>, In<sup>115</sup>, and Au<sup>198</sup> have been computed for a wide range of effective scattering per atom. Interference scattering and Doppler broadening were neglected. The method of R. Goldstein and E. R. Cohen\*\* was used. In this method the flux over the width of the resonance is represented as a linear combination of narrow and wide resonance fluxes, and that combination is chosen which makes the iterated resonance integral equal to its first estimate. The virtue of this mixed representation is that it allows more accurate treatment of resonances which are neither wide nor narrow, (e.g., the 192 ev resonance in U<sup>238</sup>) and of resonances whose practical width changes markedly with effective scattering.

#### B. Reactor Fuels

#### 1. Corrosion Studies

a. Lightweight Alloy for Liquid Mercury - Commercially pure titanium was carburized by the decomposition of the hydrides with methane at  $1000\,^{\circ}$ C. In order to protect the reaction, an argon-methane mixture containing 10% methane by volume was used. The argon provides a rapid disposal of the reaction gas.

Corrosion test results indicate that the carburized titanium was immune to liquid mercury during four weeks exposure at 371°C. The thickness of the carburized layer will be determined metallographically. Further exposure is planned at higher temperatures in liquid mercury.

<sup>\*</sup>Rice, McQueen and Walsh, Solid State Physics, Vol. 6 (1958).

<sup>\*\*</sup>Rubin Goldstein and E. R. Cohen, Trans. American Nuclear Soc. 3, 232 (1960).

b. Zirconium Alloys for Superheated Steam - There has been no appreciable change in the behavior of the copper-iron-nickel alloys tested at  $540^{\circ}$ C (~110 days) and  $650^{\circ}$ C (~90 days) under a pressure of 600 psi. However, the tests at  $650^{\circ}$ C have been discontinued because of heavy oxide buildup particularly at the rims of the disc shaped samples.

A titanium-containing alloy tested at 540°C showed increasing absorption of corrosion product hydrogen (expressed as ratio of hydrogen absorbed to hydrogen produced) with time. It is probable that the film became thick enough so that it was no longer an electronic conductor. The concept upon which these alloys were designed requires that the corrosion product film be an electronic conductor. Recent data indicates that iron is more suitable for promotion of electronic conductivity in the corrosion product film.

c. Ferrous Alloys for Superheated Steam - 406 stainless steel continues to be much superior to types 304, 316, and 347 after about 90 days at 650°C and 600 psi. 406 shows small weight gains. The 300 series materials are covered (at least partly) with spalling oxide.

#### 2. Ceramic Fuels

a.  $\underline{\text{UC-PuC Bodies}}$  - Preparation and fabrication techniques for UC are being investigated as a program complementary to the work on PuC. Techniques which can be transposed to PuC preparation and fabrication are of most interest. To date most of the work has been directed toward the preparation of UC.

Two methods of preparation are being investigated; (a) reaction of UO<sub>2</sub> with carbon in flowing argon at a temperature of  $1400^{\circ}$ - $1500^{\circ}$ C, and (b) the reaction of UO<sub>2</sub> with carbon in a plasma flame at temperatures above the melting point of UC. The first method requires reaction times of the order of one to two hours at temperature; the latter requires only a fraction of a second reaction time for particles of the order of 100 microns in diameter.

The first method consists of dissolving petroleum pitch (the carbon source) in a solvent such as benzene and mixing the solution with  $UO_2$ . After mixing, the material is in the form of a thick slurry. After evaporating the solvent at room temperature the material is pulverized and can be fired as a powder or formed into pellets before firing in argon.

The first stage in the firing is the carbonization of the pitch which begins at approximately 400°C and is complete at 950°C. The second stage of firing is the reaction of the residual carbon with the  $UO_2$  which begins at approximately 1300°C and reacts to completion fairly rapidly at 1450°C.

Chemical analyses on this material gave average values of 93.46% U, 6.22% C, and 0.09%  $O_2$ . X-ray diffraction examination revealed the predominant phase to be UC with some UC<sub>2</sub> present. None of the reflections for UO<sub>2</sub> were detectable.

The second method consists of preparing the  $UO_2$ -C mixture in the form of a sized powder and passing this material through a plasma flame into a receptacle containing an inert atmosphere. The most satisfactory method of preparing a feed material is to make a slurry of  $UO_2$  and pitch-solvent solution, allow the solvent to evaporate at room temperature, pulverize the dry material, and carbonize the resultant powder in an inert atmosphere. The carbonized material is crushed and sized to control the particle size of the reacted product and also to produce a free-flowing powder.

Work is still in progress on this technique of preparation to establish the various parameters which control the quality of the final product. To date the best carbide produced has been approximately 60% UC and 40% UO<sub>2</sub> with probable nitrogen contamination of the carbide. This was achieved using a nitrogen flame 6 in. long with a flowing argon atmosphere in the receptacle. There is now available plasma flame equipment which will produce a helium flame 12 to 15 in. long. It is thought this new equipment will allow the necessary flexibility to produce a good quality monocarbide.

Plutonium carbide, and mixtures of plutonium and uranium carbides, have been formed by mixing the oxides with pitch and, after decarbonization of the pitch, reacting at  $1450^{\circ}\text{C}$ . Plutonium carbide formed in this manner was found to consist predominantly of PuC with  $\text{Pu}_2\text{C}_3$  as a major contaminant. The uranium-plutonium oxide mixtures which were reacted to the carbide were found to consist of a mixture of PuUC and residual oxide. The material produced by this reaction was crushed and compacted into pellets or cylinders and sintered at  $1750^{\circ}\text{C}$  for 30 minutes. These pellets had a geometric density of 80 to 83% of theoretical. Individual grains, however, in these pellets were found to have densities above 92% of theoretical, and the pellets contained a large number of open pores.

b. <u>Uranium Oxide Binary Systems</u> - The uranium oxide-lanthanum oxide system was investigated to determine the phase relationships under a variety of experimental conditions. Compositions of known metal atom concentrations were subjected to oxygen, air, hydrogen and vacuum environments at elevated temperature conditions. The volatility behavior of the urania-lanthana solid solutions was studied. Specimens containing more than 60 m/o LaO $_{1.5}$  had very low weight losses and their loss rates were

nearly constant. Microstructure examination indicated that grain growth and densification had occurred and that the specimen surfaces were relatively inert to attack by the furnace gases. Specimens within this range had O/M ratios below the stoichiometric  $MO_{2,\,00}$  composition and were the most stable with regard to volatility behavior.

High urania specimens containing 20 to 50 m/o  $\rm LaO_{1.5}$ , however, had much higher weight losses and their exposed surfaces appeared to be attacked by the furnace gases. Microstructure examination indicated that the excessive weight losses are accompanied by increases in open porosity near the exposed surfaces. Attack of high urania specimens appears to occur by urania vaporization along grain boundaries. A decrease in the volatility rate was noted after long exposure and may be caused by vapor saturation within the porosity channels. The O/M ratios of these volatile compositions were in excess of 2.10.

The transition between volatile and nonvolatile compositions (55 to 60 m/o  $LaO_{1.5}$ ) had intermediate surface attack and weight losses. The O/M ratios of these compositions were between 2.07 and 2.01.

The extremely low volatility of compositions containing more than 60 m/o  $\rm LaO_{1.5}$  cannot be explained adequately as a dilution effect resulting from the substitution of lanthanum for uranium. This consideration would result in a linear relation between urania loss and lanthana concentration. The stoichiometry differences between volatile and nonvolatile compositions, however, leads one to an alternative explanation. Solid solutions containing more than 65 m/o  $\rm LaO_{1.5}$  have oxygen to metal atom ratios below the stoichiometric  $\rm MO_{2.00}$  composition. Specimens exhibiting appreciable vaporization, however, have stoichiometries in excess of 2.00. The change from an oxygen-deficient to an oxygen-excess structure appears to be a significant factor in the volatility behavior of these solid solutions.

The following conclusions have been drawn concerning this system:

- 1. Cubic fluorite solubility extends over a considerable portion of the uranium oxide lanthanum oxide system.
- 2. The stoichiometries of solid solutions having identical metal atom contents can be varied over considerable limits by subjecting the compositions to vacuum, hydrogen, and oxidizing environments at elevated temperatures.
- 3. Substoichiometric solid solutions tend to oxidize in air at room temperature toward the stoichiometric  $MO_{2.00}$  composition. The ease of oxidation apparently depends upon the  $U^{4+}$  content and on the degree of substoichiometry.

- 4. The variation in lattice parameter with O/M ratio for a 50 m/o  $\rm LaO_{1.5}$  composition suggests that two different mechanisms govern the accommodation of oxygen in the cubic fluorite structure.
- 5. Solid solutions containing more than 65 m/o  $LaO_{1.5}$  have oxygen-deficient structures when subjected to oxidizing environments. The uranium constituents of these solid solutions are in the  $U^{6+}$  state.

Uranium oxide-neodymium oxide binary systems have also been studied. Different U-Nd-O compositions were sintered in air and hydrogen at 1650°C for four hours. Solid solutions were readily formed in air within the approximate composition limits of 20-60 m/o NdO<sub>1.5</sub>. Mixtures of UO<sub>2</sub> and NdO<sub>1.5</sub> when sintered in hydrogen were found to form solid solution at a slower rate than corresponding compositions which were sintered in air. In some instances solid solutions were incompletely formed by the heat treatment at 1650°C in hydrogen.

At low NdO<sub>1.5</sub> concentrations the UO<sub>2</sub> fluorite type structure can be distinguished up to 30 m/o NdO<sub>1.5</sub>. These solid solutions were found to have lattice parameters of 5.470  $^{\rm t}$  0.001Å which is close to that of pure UO<sub>2</sub>. A different face centered cubic solid solution (reversal solution) in this region was also observed. These solutions had smaller lattice parameters (5.448 - 5.450Å) which increased slightly as the NdO<sub>1.5</sub> content increased. Between 30 to 60 m/o NdO<sub>1.5</sub> only one solid solution was found to be present with a lattice parameter which increased from 5.455 to 5.498Å. At 70 m/o NdO<sub>1.5</sub> a second face centered structure was observed with a lattice parameter of 5.521Å. This lattice size is very close to the size of the cubic substructure of the "C" type rare earths (5.53Å). At 80 m/o NdO<sub>1.5</sub> the predominant phase observed was the "C" type rare earth structure. A small amount of a hexagonal phase was present which was probably due to the hydrolysis of NdO<sub>1.5</sub>. Beyond 80 m/o NdO<sub>1.5</sub> the hexagonal phase was found to increase as the cubic phase decreased.

c. <u>Urania-Thoria Bodies</u> - During October, work was concerned with the oxidation stability of urania-thoria solid solutions and with the effects of oxidiation and heat treatments on stoichiometry and some properties of the solid solutions.

Nonstoichiometric solid solutions were prepared by air sintering  $\rm U_3O_8\text{--}ThO_2$  compositions containing a maximum of 70 m/o  $\rm UO_2$  equivalent. This compositional range was chosen since it has been shown that approximately 70 m/o  $\rm UO_2$  equivalent is the upper limit of the single phase solid solution region for air sintered materials. Solid solutions were formed by reacting the materials at either 1500°C or 1650°C for 18 hours. Solid solution formation was confirmed by X-ray diffraction.

There was no detectable difference in stoichiometry, as determined from weight change calculations, as a result of increasing the reaction temperature from  $1500^{\circ}\text{C}$  to  $1650^{\circ}\text{C}$ . As an indication of the degree of stability, solid solutions formed by air sintering were reduced in hydrogen and reoxidized by heating for 100 hours at  $1000^{\circ}\text{C}$  in a flowing oxygen atmosphere. The departure from stoichiometry increases rather uniformly with increasing uranium oxide content. Compositions containing less than  $10~\text{m/o}~\text{UO}_2$  are nearly stoichiometric (U.05 Th.95O2.03) and weight loss calculations indicate that these compositions are susceptible to volatilization losses during sintering. The results of the reduction-reoxidation treatment indicate that the degree of nonstoichiometry resulting from the long-time sintering in air is a near-equilibrium value. The stoichiometry following this treatment was nearly identical to that obtained as a result of air sintering indicating the degree of oxidation was reversible.

The cell sizes for materials prepared by air sintering and by reduction-reoxidation of these solid solutions are in close agreement although there is a tendency for reoxidized materials to have a slightly larger cell size indicative of a higher degree of oxidation. Cell sizes determined for solid solutions formed by air sintering at 1500°C followed by  $\rm H_2$  reduction at 1000°C are in close agreement with theoretical values for the system  $\rm UO_2\text{-}ThO_2$ . The disagreement of  $\rm H_2\text{-}reduced$  values with the theoretical curve is probably due to urania volatilization during sintering especially in the region of 2.5 to 10 m/o  $\rm UO_2$  where weight loss determinations indicated volatilization.

d. <u>Uranium-Thorium Sulfide</u> - Work continued on evaluation of the solid solution bodies which consisted of US-ThS mixtures with molar ratios of 100:0, 75:25, 50:50, 25:75 and 0:100 fired at 1805°, 1935° and 2050°C.

Chemical analyses of the 1935°C series showed that the monosulfide phase decreased from 99.6 w/o for US to 97.0 w/o for ThS, the remainder being oxide or oxysulfide. The S/metal ratio also decreased from 0.963 for US to 9.920 for ThS.

Polished sections were made of the solid solution series at all three temperatures and the following general observations were made:

(a) <u>Unetched 1805° and 1935°C Series</u>: US showed a very small amount of secondary phase as small discrete particles; the solid solution members showed the secondary phase as large agglomerates with a general crystal plane orientation while ThS showed it as more of a needlelike Widmanstätten precipitate. All sections appeared quite porous with small grain size.

- (b) <u>Unetched 2050°C Series</u>: US appeared the same as in the other two series. As the solid members approached ThS the secondary phase changed from small particles on crystal planes to Widmanstätten needles at ThS. In all cases (excepting US) the secondary phase clearly defined the boundaries of large dense grains.
- (c) Etching Effects  $(10 H_2 O_2: 1 H_2 SO_4)$ : All three US samples showed the Widmanstätten groove etching mentioned in the July Progress Report (ANL-6399). None of the solid solution members showed this effect. US-rich phases appeared gray in the etched sections while ThS-rich phases appeared white. Because of this, it was possible to confirm the X-ray results visually, which indicated solid solution was not complete until 2050°C.

Vicker's hardness measurements made on the polished sections before etching showed even softer US than measured previously. The 2050°C series, considered the most reliable, gave a VPN of 184 for US increasing to 277 for  $\rm U_{0.5}Th_{0.5}S$ , then dropping to 234 for ThS.

To test compatibility with reactor environment, US discs were clamped in intimate contact with cladding materials and immersed in NaK at 800°C for two weeks. Polished sections showed no reaction or only a negligible reaction of the US with NaK, stainless steel, vanadium or niobium; however, there was a reaction zone of about 0.7 mils between zirconium and US. Irradiation tests will be made as soon as possible.

Powdered US from the solid solution series was run in the DTA apparatus using a dynamic  $O_2$  flow through the sample. Rapid oxidation began at 375°C characterized by three strong exothermic peaks in rapid succession. ThS run under the same conditions showed rapid oxidation beginning at 500°C with only two exothermic peaks. The solid solution members are now being run.

# 3. Nondestructive Testing

a. Neutron Techniques - The excellent image sharpness now available with the use of gadolinium screens in direct exposure neutron radiography has encouraged several application studies employing this technique. One such study, for example, has involved the inspection of hydrogenous material such as wood and adhesives.

The specific object involved in the adhesive inspection study was an aluminum skin, adhesive bonded honeycomb panel such as those used in aircraft construction. Because of the high neutron absorption of the adhesive and the low neutron absorption of the other materials present,

neutron radiographic methods rather easily display the location and structure of the adhesive within the panel. By such means, it should be possible to determine whether or not the adhesives are located in the desired areas of the assembled panel.

A second general type of inspection problem which lends itself to neutron radiography is illustrated by the inspection results obtained with a zirconium clad, sintered boron carbide poison element. Among the inspection problems encountered with such material is that of determining the uniformity of distribution of the boron carbide within the bar of material. This is a relatively simple problem for neutron radiography because of the high neutron absorption of the boron. By X-ray techniques, however, it is a difficult task because the X-ray absorption by all the materials present in the sample is so similar. This is an excellent practical illustration of how neutron radiographic inspection can be useful.

A third application study (as yet unsuccessful) is concerned with the possibility of locating areas of hydrogen concentration within metals. The specific objects investigated include single crystal zirconium samples and Zircaloy tubing. The resolution of the imaging system in each case did not seem sufficient to yield the desired information. Further efforts to improve this characteristic are now in progress.

b. Eddy Current Techniques - Development work has continued on the pulsed-field reflection system mentioned in the Progress Report for January, 1961 (ANL-6307). This electromagnetic test method replaces the sinusoidal currents and test coils or probes of the older eddy current test system with pulsed fields emanating from small apertures in special masks. Test information about the metallic specimen being examined is received as a series of reflections from the surface and from inside the metal. This system represents a possible new approach to the problems of the electromagnetic testing field. Recently it was discovered that the pulsed-field reflection system in its present form possesses a pronounced sensitivity to the orientation of flaws in the metal passing under the aperture. The mask-aperture-pickup assembly can be oriented to achieve maximum pickup of defects of one orientation while minimizing all others.

Experiments are in progress which are designed to produce a better understanding of this effect, and how it can best be used in practical test situations. Artificial defects produced by a discharge cutting machine are being used in these experiments because their orientation with respect to the aperture is known in advance. Tests are being made on samples of 1 in. OD x 0.020 in. wall Zircaloy-2 tubing. These sample sections contain defects which have been discovered by ultrasonic tests. Ultrasonic methods are useful on this tubing because of its exceptionally smooth ID and OD surfaces. Internal defects indicated by the ultrasonic method are readily detected by the pulsed field reflection system, and an

effort is being made to determine the orientation of these defects from information derived from the artificial defect experiments. These predictions will be checked by taking metallographic sections of the defective area.

#### C. Heat Engineering

## 1. Double Tube Burnout Study

The double tube burnout test is an attempt to produce constant exit steam quality burnout data. This test is to be run with an annular test section in which the inner and outer tubes are heated independently with separate power supplies. By increasing the power on one tube while decreasing it on the other, a constant total power (and constant quality) can be maintained even though the heat flux is being varied.

The preliminary test section has been installed in the experimental loop and debugging of the equipment is underway. The flow measurement and temperature measurement instrumentation has been checked and is operating satisfactorily. The Wheatstone bridge-type burnout detectors, which have operated satisfactorily with single tubes, had to be rejected for this test because of the inability to eliminate a-c pickup resulting from the interacting fields of the two power supplies. Tests are being run on burnout detectors that use thermocouples to detect the temperature rise in the tube wall at the time the burnout occurs. The power recording instrumentation was also plagued with a-c pickup problems but it is thought that this can be eliminated by proper filtering.

# 2. Hydrodynamic Computer Program

A digital computer program that will permit a complete steadystate hydrodynamic calculation of almost any conceivable boiling reactor core geometry is being prepared for the IBM-704 computer (see Progress Report for September 1960, ANL-6234, for program description). Actual programming of the equations has been started.

# 3. Hydrodynamic Instability

The analog computer program describing the transient response characteristics of a forced circulation two-phase loop was wired and operated. The results compare favorably with experimental measurements from the Armadilla test loop.

A momentum conservation equation balancing friction and acceleration against net driving head was substituted for the pump portion of the above analog program. The resultant program described the transient

response characteristics of a natural circulation loop. This program was compared with the experimental results from the Armadilla test loop at steady state conditions and with a sinusoidally varying input power of frequency 0.5, 1 and 2 cycles per second. Again the experimental results compared favorably with the analog results.

Restriction tests at 41 atm (600 psia) and at 27 atm (400 psia) have been analyzed for the stabilizing influences of test section inlet restriction on the inception of hydrodynamic instability. A new series of tests on a 2.38-cm ID test section are planned to provide further information on the influence of restrictions on stability thresholds to confirm results obtained to date.

A test to vary inlet flow on the small-scale loop has been scheduled to follow the preliminary tests of the double-tube burnout test section.

## 4. Critical Heat Flux Survey

An improved correlation for the prediction of the critical heat flux occurrence during the nucleate boiling of water has been synthesized from the empirical equation of Jens and Lottes, the dimensionally-analyzed Kutateladze equation, and various bodies of critical heat flux data. The correlation is of the form:

$$Q"/10^6 = \frac{(H_{fg}/10^3)(G/10^6)^n}{D_{e}^{1/2}} [f (H_{f} - H_{local})]$$

where

 $Q'' = critical heat flux - Btu/(hr)(ft^2)$ 

G = mass flow rate -  $lb/(hr)(ft^2)$ 

De = flow channel equivalent diameter - in.

H<sub>fg</sub> = latent heat of vaporization - Btu/lb

H<sub>F</sub> = enthalpy of saturated liquid water - Btu/lb

H<sub>local</sub> = enthalpy at point of critical flux - Btu/lb

n = function of pressure-dependent fluid property

This correlation is being tested with available data from several flow geometries for wide ranges of all the pertinent variables.

# 5. Boiling from a Liquid-Liquid Interface

The purpose of this experiment is to study the process of nucleation and boiling from a perfectly smooth surface, that of mercury. Although the results are not expected to be applicable directly to a system design, this

simple experiment is expected to yield basic information and data which are needed for a better physical understanding of the boiling phenomenon and for quantitative analytical formulation of the problem.

The apparatus used and some preliminary tests were reported in the Progress Report for March 1961 (ANL-6343). Since then the heating plate has been redesigned and some earlier experimental difficulties have been successfully eliminated.

To correlate the data it is necessary to know the surface temperature of mercury. For this purpose a movable thermocouple has been developed that can measure temperatures a few thousands of an inch below the surface of mercury. The surface temperature is then obtained by extrapolation. Some data have been obtained and are now being reduced.

#### D. Separations Processes

## 1. Fluidization and Fluoride Volatility Separations Processes

a. Direct Fluorination of Uranium Dioxide Fuel - Two runs made to clarify the effect of oxygen in the direct fluorination of uranium dioxide pellets have been further analyzed. One run was made with an inert bed of aluminum oxide as a heat transfer medium. The second run was made without an inert bed. The uranium content of bed samples taken during the inert fluid-bed runs has supported preliminary indications of a relatively low oxidation rate below 400°C and a high rate at 500°C and above. However, irregularities in the bed sample analyses make it doubtful that such samples are representative of the bed as a whole. Refinements of the oxygen determination procedure have been made for subsequent runs. Experiments are planned to investigate the effect of fines on fluid-bed operation.

A fluorination of the oxide residue from the run without an inert fluid bed was carried out. The center-of-the-bed temperature was used for control at  $500^{\circ}\text{C}$  ( $\pm50^{\circ}$ ) and the wall temperature averaged about  $100^{\circ}\text{C}$ . The average uranium hexafluoride production rate was 240 g/hr. The average fluorine inlet concentration was 18 percent in nitrogen. The fluorination was terminated at 5.5 hr and the bed residue examined. A light crust was noted in a vertical gas channel but the surface and the bulk of the bed were free flowing.

# b. Separation of Uranium from Zirconium-Clad and Alloy Fuels

(1) Hydrochlorination and Fixed-Bed Filter Studies Using
Uranium-Zirconium Alloys - The efficiency of a down-flow fixed-bed filter
system is being investigated in conjunction with the fluid-bed hydrochlorination of low uranium-Zircaloy alloy specimens. The overall system consists

of a  $1\frac{1}{2}$ -inch diameter fluid-bed reaction zone connected by a horizontal off-gas line (about one-foot long) to a three-inch diameter vertical pipe section which contains the granular material (alundum) used as a filter-bed medium. A three-inch deep filter-bed was used in the current studies. Increased velocity (in the range 0.23 to 0.75 ft/sec) through the filter-bed had no apparent adverse effect on filtration efficiency as determined by uranium losses from the system. Typical uranium losses from the combined fluidized reaction bed and fixed-bed filter system (Norton Alundum, Type 38 in both cases) were 0.14 and 0.17 percent for velocities of 0.28 and 0.75 ft/sec, respectively. The initial charges, 9.9 and 3.2 g of uranium as 2.74 weight percent uranium-Zircaloy alloy, were hydroclorinated at temperatures of 350° to 400°C using 13 and 44 mole percent hydrogen chloride in nitrogen.

Calculations based on the chloride, uranium and zirconium content of the reaction- and filter-beds indicate that little, if any, chloride is associated with the relatively large amounts of inert material. Thus there should not be excessive fluorine consumption in the subsequent step.

- (2) <u>Fluid-Bed Fluorination Studies</u> An operationally satisfactory shakedown run carrying out the hydrochlorination and fluorination steps successively was made using Norton, Type 38 Alundum for the reaction and down-flow filter beds. Temperatures near 400°C were used in both steps.
- (3) Fluid-Bed Hydrolysis of Zirconium Tetrafluoride Methods are being examined for processing zirconium tetrachloride, which is a gaseous waste stream of the hydrochlorination of low uranium-zirconium alloy fuel. Initial studies involve reaction of the tetrachloride with steam to produce zirconium dioxide. The reaction is conducted in a heated fluid-bed reactor, and the oxide is expected to be deposited as a coating on the bed particles. Nitrogen and steam are used as the fluidizing gas. Preliminary trials conducted in a six-inch diameter unit using zirconium tetrachloride sublimed in a tube furnace as feed gas were only partially satisfactory due to plugging of the entrance line. Equipment modifications are in progress.
- (4) Fluoride Separations Several solids have been considered for use as inert, fluidizable bed materials for the fluorination step of the Direct Fluorination Volatility Process. Refractory alumina, of high purity, has shown the most promise for this use. The addition to the alumina of about one percent nickel fluoride (to simulate corrosion products) and 0.5 percent zirconium tetrafluoride (present from a prior decladding step or as a fission product), did not hinder the removal of uranium and plutonium from the solids upon fluorination. Where aluminum fluoride was substituted for the alumina, the retention of plutonium in the aluminum fluoride, after fluorination at 450°C for ten hours, was greater than that observed

for alumina. The plutonium concentration in the residual aluminum fluoride was 0.18 percent whereas in the alumina in similar experiments it had been reduced to 0.02 percent from an original concentration of one percent of the bed weight.

Experiments are being made to determine the efficiency of removal of plutonium particulate matter from the exhausts of ventilation systems. There is concern with the prevention of release of plutonium hexafluoride from experimental facilities to the atmosphere. Controlled releases of uranium and plutonium hexafluoride are being made in small-scale experimental equipment into air having a controlled moisture content. The air stream is passed through an AEC type filter medium to determine the efficiency of uranium and plutonium removal. No conclusions have yet been drawn.

Iodine has been reacted with plutonium hexafluoride at 25°C to produce iodine pentafluoride, plutonium trifluoride and plutonium tetrafluoride. The rate of the reaction is not yet known. Plutonium hexafluoride has been reacted with mercury but quantitative information is not yet available. Plutonium tetrafluoride does not appear to react with aluminum fluoride at 700°C.

## 2. General Chemistry and Chemical Engineering

- a. Conversion of Uranium Hexafluoride to Uranium Dioxide Two-Step Fluid-Bed Process
- (1) Steam Hydrolysis of UF $_6$  to UO $_2$ F $_2$  A run was made in an attempt to extend continuous run time for the steam hydrolysis of uranium hexafluoride to uranyl fluoride in a three-inch diameter fluid-bed reactor. Operating conditions were 100 g/min hexafluoride feed, 200° to 230°C bed temperature, 0.8 ft/sec steam superficial gas velocity (245 percent steam excess) and a solids recycle rate equivalent to 15.6 percent of the uranium hexafluoride feed rate. Average bed particle size was maintained in the range 317 to 366 microns. The feasibility of operating this reaction system continuously for extended periods is now more firmly attributed to the technique of allowing fines produced in the bed either by attrition or gas phase reaction to be entrained from the reactor. In previous operations fines were returned to the bed during filter blowback. The filters are now contained in a separate vessel. The run time has been extended to 25 hours, terminating at the end of this period upon exhaustion of the feed cylinder.
- (2) Fluid-Bed Calcination Studies in Small-Diameter Columns—Studies to extend fluid-bed calcination techniques to systems involving criticality considerations are being continued. Successful runs of five hours and seven and one-half hours have been made in the newly modified small diameter ( $2\frac{1}{4}$ -inch) calciner. Two porous metal filters in parallel replaced

the single filter in the disengaging section. The longer run was deliberately interrupted after five hours by a shutdown and startup procedure and then continued for an additional two and one-half hours.

(3) Preparation of Uranium Carbide - The effect of agitation on the preparation of uranium carbide by precipitation from liquid metal solutions was investigated. It was found that adequate stirring speeds and baffles in the vessel are necessary in order to obtain satisfactory reaction rates.

An attempt was made to coprecipitate uranium and cerium carbides by adding carbon to a zinc-10 weight percent magnesium solution of uranium and cerium. About 99 percent of the uranium precipitated whereas nearly all of the cerium remained in solution.

## 3. Chemical-Metallurgical Process Studies

a.  $\underline{\text{Liquid Metal Solvent Studies}}$  - The solubility of praseodymium in liquid zinc may be represented by the empirical equation

praseodymium (560° to 725°C): log (atom percent) =  $7.469 - 7711 \text{ T}^{-1}$ 

The solubility of vanadium in liquid zinc may be represented by the equations

vanadium (450° to 623°C): log (atom percent) =  $7.260 - 10010 \text{ T}^{-1}$ +  $3.086 \times 10^6 \text{ T}^{-2}$ vanadium (623° to 670°C): log (atom percent) =  $0.9652 - 925.6 \text{ T}^{-1}$ 

vanadium (670° to 756°C): log (atom percent) =  $-1.045 + 969.7 \text{ T}^{-1}$ 

The retrograde solubility of vanadium in zinc above  $670^{\circ}\text{C}$  was confirmed (see Progress Report for July, 1961, ANL-6399).

Epsilon zinc-uranium crystals were formed in a saturated zinc matrix by annealing a 21.5 weight percent uranium-zinc mixture at 800°C for 18 days in a sealed tantalum capsule. Chemical analysis of the crystals, which were recovered from the ingot by electrolytic etching, showed the composition to be 28.2 weight percent uranium and 72.1 weight percent zinc. This corresponds to a zinc-uranium atom ratio of 9.31. The uranium content of the crystals obtained in this experiment is higher than the uranium content (25.9 weight percent) of crystals obtained in an earlier experiment (see Progress Report for April, 1961, ANL-6355). The present results indicate that the composition width of the epsilon field at 800°C is rather narrow and is closer to the composition of the delta phase (zinc-uranium atom ratio of 8.5) than had been indicated by previous tests.

A study of the coprecipitation characteristics of cerium, ruthenium, and zirconium when carried by uranium in magnesium-zinc solutions has been started. This study is important to the understanding of both the skull reclamation process and the blanket process in which uranium is precipitated from high (about 50 percent) magnesium-zinc solutions. The first experiment was designed to obtain data for several elements under conditions similar to those encountered in the skull reclamation process. A solution containing 10 percent uranium, 12 percent magnesium, 77 percent zinc, 0.17 percent zirconium, 0.03 percent ruthenium and 0.7 percent cerium was prepared at 800°C. Magnesium was then added to bring the magnesium content of the solution to about 53 percent. This addition of magnesium resulted in a substantial precipitation of uranium. The system was cooled from 800°C to 400°C and samples of the liquid phase were taken at about 50-degree intervals. Preliminary results indicate that (1) cerium does not coprecipitate with uranium, (2) zirconium may coprecipitate under certain conditions, and (3) ruthenium does coprecipitate with uranium.

A decrease in zirconium concentration occurred at  $800^{\circ}\text{C}$  when magnesium was added to make the 53 percent magnesium-zinc solution. This decrease is attributed to coprecipitation of zirconium with uranium. Cooling the solution from  $800^{\circ}$  to  $557^{\circ}\text{C}$  produced no further reduction in zirconium concentration even though the amount of uranium in solution decreased by a factor of about four. Over this temperature range the uranium which is being precipitated changes from  $\gamma$ - to  $\beta$ -uranium at about 772°C and from  $\beta$ - to  $\alpha$ -uranium at  $665^{\circ}\text{C}$ . Most of the uranium precipitated is either  $\beta$ - or  $\alpha$ -uranium. The data, therefore, suggest that coprecipitation of zirconium by  $\beta$ - and  $\alpha$ -uranium is less than by  $\gamma$ -uranium. A decrease in zirconium concentration observed below  $557^{\circ}\text{C}$  is attributed to the precipitation of a zirconium-zinc intermetallic phase.

Ruthenium appeared to coprecipitate with  $\gamma$ -,  $\beta$ -, and  $\alpha$ - uranium. The data suggest, however, that there is a difference in coprecipitation of ruthenium by  $\gamma$ - and  $\beta$ -uranium.

Further studies of the coprecipitation of zirconium and ruthenium by  $\gamma\text{-}$  and  $\beta\text{-}\text{uranium}$  will be made to confirm the present findings.

The solubility of uranium in 53 percent magnesium-zinc solution over the temperature range of  $450^\circ$  to  $800^\circ$ C may be represented by the equation

log (weight percent uranium) =  $1.629 - 2245 \text{ T}^{-1}$ 

The codistribution of uranium and plutonium between liquid lead and zinc was determined at several temperatures. The values of the individual distribution coefficients, K, (K = amount of solute in zinc layer/amount of solute in lead layer) were found to be as follows: at 700°C, U = 52.1,

Pu = 16.4; at  $730^{\circ}$ C, U = 27.3, Pu = 8.9; at  $765^{\circ}$ C, U = 10.8, Pu = 5.1. The values for the distribution coefficient for uranium obtained in this study agree well with values obtained recently for uranium alone in a similar solvent system. The values for the distribution coefficient of uranium alone were found to be  $55 \pm 5$  at about  $700^{\circ}$ C and  $29 \pm 3$  at about  $730^{\circ}$ C.

Study of the lanthanum-cadmium system by means of the recording effusion balance has shown the existence of the following phases:  $LaCd_{11}$ ,  $LaCd_{5}$ ,  $LaCd_{2}$ , and LaCd.

b. <u>Calorimetry</u> - A series of combustions of zirconium hydride in oxygen has yielded the value  $\Delta E_{\text{C}298}^{\circ}$  = -3093.85  $^{\frac{1}{2}}$  1.58 cal/g for the standard energy of combustion. The heat of formation of zirconium hydride was calculated to be  $\Delta H_{\text{f}298}^{\circ}$  = -40.46  $^{\frac{1}{2}}$  0.41 kcal/mole. Similar calorimetry for zirconium deuteride in oxygen gave the values  $\Delta E_{\text{C}298}^{\circ}$  = -3039.80  $^{\frac{1}{2}}$  1.25 cal/g and  $\Delta H_{\text{f}298}^{\circ}$  = -41.51  $^{\frac{1}{2}}$  0.37 kcal/mole. In the combustions, the hydride and deuteride were encapsulated by means of the polyester film, Mylar. A value of  $\Delta E_{\text{C}298}^{\circ}$  = -5477.19  $^{\frac{1}{2}}$  1.03 cal/g was obtained for the standard energy of combustion of Mylar.

Calorimetric combustions of silica glass in fluorine were found to yield  $O_2$  and  $\mathrm{SiF}_4$  as products. A series of six runs yielded a value of  $\Delta E_{C~298}^{\circ}$  = -2830.0  $\pm$  0.4 cal/g of silicon dioxide for the standard energy of combustion.

A preliminary series of calorimetric combustions of magnesium in fluorine has been started. Experiments to establish optimum sample size, fluorine pressure, and sample orientation for maximum combustion are being carried out.

Work is continuing on the combustion of uranium in fluorine. A method of selectively determining the amounts of uranium metal and uranium trifluoride in the presence of other uranium fluorides is being developed.

The drop mechanism of the high-temperature enthalpy apparatus has been assembled apart from the calorimetric system. Performance of the mechanism and drop speeds are being determined.

# E. Advanced Reactor Concepts

# 1. Fast Reactor Test Facility (FARET)

The general engineering and physics parameters for an experimental facility to test advanced fast reactor cores are being examined to prove the feasibility of a generalized test facility.

a. Facility Design - A reactor vessel design concept has been completed in which the core support plate is removable and the control rod spacing adaptable to various experimental core designs. Fuel removal is by means of two rotating plugs, avoiding the use of a transfer arm. After lifting a fuel assembly, the rotating plugs index the assembly directly over a transfer basket. The fuel assembly is then lowered into the transfer basket. A removal tool is used to cap the basket and to lift the basket up and into the fuel handling cask.

Another approach to fuel handling is being studied in which each fuel assembly is extended by a shielded section, so that the fuel elements will be readily accessible through a relatively thin cover. This method would allow more flexibility for installation of instrumentation in subassemblies for the direct measurement of parameters such as flow, temperature, and pressures.

b. Heat Transfer, Fluid Flow, Stress Analysis - Calculations were made for an AISI Type 316 stainless steel U-shell, U-tube intermediate heat exchanger with sodium on the primary side and NaK on the secondary side. This was done for the primary fluid flow rate of 380 liters/sec, an inlet temperature of 760°C (1400°F), and a power level of 50 Mw. The design criterion is the limitation of the temperature gradient in the tubes in order to restrict the stresses to ASME allowable values. This results in absorbing the major system-to-heat sink temperature difference in the air-cooled finned heat exchanger in the secondary system.

The intermediate heat exchanger baffle geometry would be designed to promote shell-side cross flow and minimize bypass streaming. The results of the calculations are as follows:

No. of tubes, 0.75 in. dia. (2 cm)	545
Total surface	3600 ft <sup>2</sup> (330 m <sup>2</sup> )
Log mean temperature difference	21°C
Primary fluid inlet temperature	760°C
Primary fluid outlet temperature	518°C
Secondary fluid inlet temperature	497°C
Secondary fluid outlet temperature	739°C
Primary (shell) side pressure drop	$14 \text{ psi } (1 \text{ kg/cm}^2)$
Secondary (tube) side pressure drop	13 psi (0.9 kg/cm <sup>2</sup> )

Pressure loss in the remainder of the primary loop excluding the reactor was estimated to be 14 psi (l  $\rm kg/cm^2$ ). This system thus is not adaptable for gravity flow discharge from the reactor because of the relatively high primary system pressure losses. The gravity flow scheme is being studied.

#### 2. Direct Conversion for Mobile Systems

As a first approach to finding new ways to use nuclear energy for surface transportation, reactors for the production of chemical fuels suitable for either internal combustion engines or fuel cells are being considered.

The energy-producing reaction in a converter using chemical fuels is exothermic and the regeneration, or processing, reaction is endothermic. The promotion of chemical reactions by radiation is due to the formation of various hyperactive intermediate species such as ions, excited molecules and free radicals. It is the formation of a greater number of these active species at a given temperature than would otherwise exist due to thermal effects alone which causes faster reaction rates.

Of interest is the possible energy efficiency for the decomposition of light element oxides by radiation. The percentage of fission energy which finally appears as chemical energy in the fuel is given by  $G\Delta Hx/23$  where,

G = (molecules produced/100 ev absorbed)

 $\Delta H$  = heat of endothermic reaction in kcal/mole

 $\mathbf{x}$  = fraction of fission energy released in chemical reactants (fission recoils and nuclear radiations)

The  $\Delta H$  for the decomposition of alumina is 399 kcal/mole. If we assume a G value of 5 for this endothermic reaction, and an x = 0.2 (attainable with highly enriched oxide fuel particles 3 microns in diameter) then the over-all energy conversion efficiency given by the above expression is 17%. The energy efficiency for the electrochemical refining of aluminum is 40%, and assuming an electric power plant efficiency of 35% the conversion of fission to chemical energy would be 14%. Thus, the radiation-promoted decomposition process looks attractive, even at relatively low values of G, providing  $\Delta H$  is large enough. G values between 2 and 5 are currently of interest. The G values for some solid inorganic compounds are shown in Table VIII.

Table VIII. Yields of Solid-Phase Radiolysis

Reaction	Yield	Radiation
$NaN_3 - Na^+ + \frac{3}{2} N_2 + e^-$	$G(N_3^-) = 2*$	x-rays
$CsNO_3 - CsNO_2 + \frac{1}{2}O_2$	$G(NO_2) = 2G(O_2) = 1.7$	$\gamma$ -rays, x-rays
$LiNO_3 \rightarrow LiNO_2 + \frac{1}{2}O_2$	$G(NO_2^-) = 2G(O_2) = 0.02$	γ-rays, x-rays
KClO <sub>3</sub> - KCl, KClO <sub>2</sub> , KClO, O <sub>2</sub>	$G(C1O_3^-) = 3$	γ-rays, x-rays
	$G(O_2) = 3$	
KClO <sub>4</sub> → 0.7 KClO <sub>3</sub> + 0.3 KCl + 0.950 <sub>2</sub>	$G(C1O_4^-) = 5$	x-rays
	$G(C1O_3^-) = 3.5$ $G(11^-) = 1.5$	

<sup>\*</sup>For the reaction occurring at -200°C.

# 3. Compact High Power Density Reactors

The purpose of this work is to develop a compact high power density fast reactor using sodium vapor as the working fluid in a direct cycle system. Problems have been defined that will require test programs in the following areas:

- (a) The development of a structural material to function in sodium vapor at a temperature of 1000°C.
- (b) The investigation of the thermodynamic properties of sodium vapor.
- (c) The development of a method for cooling the turbine blades.
- (d) The design and testing of a sodium vapor turbine.

The conceptual design is for the equipment to modify EBR-I for a compact, 11-liter core test. The core power has been estimated at 1.0 Mw. The compound fuel element originally specified has been changed to a rod type fuel element for easier fabrication; however, this caused a reduction in heat transfer surface by approximately 25%.

## 4. Supercritical Pressure Water Reactor Study

A study of supercritical reactors is being made to accomplish the following:

- (a) To determine the maximum power capability of a supercritical water-cooled reactor core based on the largest pressure vessel that can be fabricated for the required pressures.
- (b) To review the present state of supercritical water technology for application to nuclear reactors.

The initial studies indicated that the maximum plant output would be less than 300 Mwe, but this value was based on a 9-in. (22.9 cm) thermal shield thickness. Investigation is being made of the thermal shield requirements which may lead toward a significant reduction in thermal shield thickness and a corresponding increase in core volume and power output. For this reason a preliminary criticality calculation was made using a multigroup DSN code. The neutron fluxes and capture gamma sources from these calculations will be used for determining the stress limits of the pressure vessel wall and the thermal shield thickness.

# 5. Organic Vapor Cycle Analysis

A study is being made of an organic-cooled reactor to generate organic vapor for use with a direct cycle power generation system. The purpose of this study is to determine the optimum operating conditions for this system.

Thermodynamic data of biphenyl in the superheated vapor range were used to examine a boiling biphenyl cycle. The net cycle efficiency was found to be 27% for an exhaust pressure of 0.5 psia and a regenerator effectiveness of 0.85.

Although the cycle efficiency is low in relation to other reactor systems, it is based on a value of the specific heat estimated to be accurate only within  $\pm 10\%$ . If the value of the specific heat used is 10% too high, the efficiency may be closer to 30%.

#### V. PUBLICATIONS

#### Papers

ITERATED SQUARE ROOT EXPANSIONS FOR THE INVERSE COSINE AND INVERSE HYPERBOLIC COSINE

Henry C. Thacher, Jr.

Mathematics of Computation, Vol. 15, No. 76, pp. 399-403 (October 1961)

#### EFFECT OF IRRADIATION ON FUEL MATERIALS

J. H. Kittel and S. H. Paine

Progress in Nuclear Energy, Series V, Metallurgy & Fuels, Vol. 3, "Basic Materials and Phenomena," 250-268, Pergamon Press, (1961). Ed: H. M. Finniston, J. P. Howe

# HOOD VENTILATION IN ARGONNE'S PLUTONIUM FUEL FABRICATION FACILITY

R. M. Mayfield and H. Bairiot

Heating, Piping and Air Conditioning  $\underline{33}$  (9) 124-129 (Sept., 1961)

DISCUSSION OF EFFECT OF LOW ALLOY ADDITIONS ON THE PROPERTIES OF URANIUM BY W. H. FRISKE, H. E. KLINE, AND M. H. BINSTOCK

S. Thomas Zegler

Trans. ASM <u>53</u> 887-888 (1961)

# ANL Reports

- ANL-5760 TWO-PHASE PRESSURE DROP IN A NATURAL-CIRCULATION BOILING CHANNEL B. M. Hoglund, R. J. Weatherhead, and T. R. Epperson
- ANL-6116 STRUCTURES AND PROPERTIES OF URANIUM-FISSIUM ALLOYS
  S. T. Zegler and M. V. Nevitt
- ANL-6289 CASTING OF EBR-II-TYPE TRANSIENT TEST ELEMENTS
  AND EQUIPMENT DEVELOPMENT
  H. F. Jelinek and P. L. Dewez
- ANL-6290 PREPARATION OF ALLOY FOR FIRST CORE LOADING OF EBR-II

  Donald C. Hampson

ANL-6299	EBR-II DRY CRITICAL EXPERIMENTS. Experimental Program, Experimental Procedures, and Safety Considerations  L. J. Koch, W. B. Loewenstein, A. Lovoff, H. H. Hooker, H. O. Monson, R. L. Ramp, and E. Hutter
ANL-6316	DEVELOPMENT OF REMOTE METALLOGRAPHIC TECHNIQUES FOR IRRADIATED MATERIALS R. Carlander
ANL-6334	STUDIES OF FAST REACTOR FUEL ELEMENT BE-HAVIOR UNDER TRANSIENT HEATING TO FAILURE.  I. INITIAL EXPERIMENTS ON METALLIC SAMPLES IN THE ABSENCE OF COOLANT  C. E. Dickerman, E. S. Sowa, D. Okrent, J. Monaweck and L. B. Miller
ANL-6338	CRITICAL STUDIES OF A DILUTE FAST REACTOR CORE (ZPR-III Assembly 31) J. M. Gasidlo, J. K. Long, and R. L. McVean
ANL-6354	A MECHANISM EXPLAINING THE INSTABILITY OF EBR-I, MARK II  R. R. Smith, R. G. Matlock, F. D. McGinnis,  M. Novick, and F. W. Thalgott
ANL-6370	CORROSION STUDIES OF TERNARY ZIRCONIUM ALLOYS IN HIGH-TEMPERATURE WATER AND STEAM R. D. Misch and C. Van Drunen
ANL-6385	POWER-TO-VOID TRANSFER FUNCTIONS Helge Christensen
ANL-6395	U.S. PARTICIPATION IN THE OEEC HALDEN REACTOR PROJECT, May 1959 to September 1960 Leonard W. Fromm, Jr.

CALCULATIONS FOR ZPR-VII FLUX-TRAP REACTORS

WITH HEAVY WATER-MODERATED CORES

E. M. Pennington

ANL-6406

